

Durham Research Online

Deposited in DRO:

10 March 2015

Version of attached file:

Accepted Version

Peer-review status of attached file:

Peer-reviewed

Citation for published item:

Ronkainen, T. and Välranta, M. and McClymont, E.L. and Biasi, C. and Salonen, S. and Fontana, S. and Tuittila, E.-S. (2015) 'A combined biogeochemical and palaeobotanical approach to study permafrost environments and past dynamics.', *Journal of quaternary science.*, 30 (3). pp. 189-200.

Further information on publisher's website:

<http://dx.doi.org/10.1002/jqs.2763>

Publisher's copyright statement:

This is the accepted version of the following article: Ronkainen, T., Välranta, M., McClymont, E.L., Biasi, C., Salonen, S., Fontana, S. Tuittila, E.-S. (2015), A combined biogeochemical and palaeobotanical approach to study permafrost environments and past dynamics. *Journal of Quaternary Science*, 30(3): 189-200, which has been published in final form at <http://dx.doi.org/10.1002/jqs.2763>. This article may be used for non-commercial purposes in accordance With Wiley Terms and Conditions for self-archiving.

Additional information:

Use policy

The full-text may be used and/or reproduced, and given to third parties in any format or medium, without prior permission or charge, for personal research or study, educational, or not-for-profit purposes provided that:

- a full bibliographic reference is made to the original source
- a [link](#) is made to the metadata record in DRO
- the full-text is not changed in any way

The full-text must not be sold in any format or medium without the formal permission of the copyright holders.

Please consult the [full DRO policy](#) for further details.

Journal of Quaternary Science

**A combined biogeochemical and paleobotanical approach to
study permafrost environments and past dynamics**

Journal:	<i>Journal of Quaternary Science</i>
Manuscript ID:	JQS-14-0026.R1
Wiley - Manuscript type:	Research Article
Date Submitted by the Author:	n/a
Complete List of Authors:	Ronkainen, Tiina; University of Helsinki, Environmental Sciences Väliranta, Minna; University of Helsinki, Environmental Sciences McClymont, Erin; Durham University, Geography Biasi, Christina; University of Eastern Finland, Environmental Sciences Salonen, Sakari; University of Helsinki, Geosciences and Geography Fontana, Sonia; University of Göttingen, Palynology and Climate Dynamics Tuittila, Eeva-Stiina; University of Eastern Finland, School of Forest Sciences
Keywords:	biomarker, n-alkane, macrofossil, permafrost, fen

SCHOLARONE™
Manuscripts

1
2
3
4
5
6
7
8
9
10
11
12
13
14
15
16
17
18
19
20
21
22
23
24
25
26
27
28
29
30
31
32
33
34
35
36
37
38
39
40
41
42
43
44
45
46
47
48
49
50
51
52
53
54
55
56
57
58
59
60

1 A combined biogeochemical and paleobotanical approach to study permafrost
2 environments and past dynamics

3 Corresponding author, e-mail address: tiina.m.ronkainen@helsinki.fi

4 **Abstract**

5 When investigating past peatland processes and related carbon cycle dynamics, it is essential
6 to identify and separate different peat environments: bogs, fens and permafrost, and their
7 historical plant assemblages. Bog peat layers contain relatively well-preserved plant material
8 for palaeoecological examination, whereas fen and permafrost peats are often highly
9 humified, which in turn constrains the reconstructions of the past plant assemblages. Here, we
10 analyzed the chemical composition of arctic peat plateau plants to create a local reference
11 training-set of plant biomarkers. After that we combined palaeobotanical, biogeochemical
12 and chronological analyses to one permafrost peat sequence collected from the East European
13 Russian tundra (67°03'N, 62°57'E) to investigate past peatland dynamics and to evaluate the
14 performance of the biomarker method in a highly decomposed permafrost environment. Our
15 results showed that the chronologically constrained macrofossil analysis provided most of the
16 essential information about the peatland succession. However, a more robust reconstruction
17 of the past peatland dynamics was achieved by combining palaeobotanical and
18 biogeochemical data sets. The similarity of the lipid biomarker distributions of the arctic and
19 boreal peatland plants also implies that any established modern biomarker training-set of
20 peatland plants could be applied universally to palaeoecological studies on peat sediments.

21 Keywords: biomarker, *n*-alkane, macrofossil, permafrost, fen, peat plateau

22

1. Introduction

Peat deposits are proxy archives for the past climate and peatland dynamics, e.g., peatland expansion and carbon accumulation (Yu *et al.* 2010). When investigating past peatland processes and related carbon cycle dynamics, it is essential to identify and separate the different peat environments (bogs, fens and permafrosts), as they differ considerably in their ecohydrology i.e., the quantity, quality and physical state of water (Wheeler and Proctor, 2000; Økland *et al.*, 2001). Consequently they maintain substantially different plant assemblages; dry hummock *Sphagnum* mosses and dwarf shrubs dominate bogs and the top parts of modern permafrost peat plateaus, whereas more water-demanding lawn and hollow *Sphagnum* mosses and sedges dominate fens and permafrost peat plateau depressions (e.g. Oksanen *et al.*, 2001; Rydin and Jeglum 2006; Virtanen and Ek 2013). Remnants of these different peatland assemblages in historical peat deposits make it possible to separate different peatland environments when reconstructing peatland dynamics back in time (Yu *et al.*, 2013). Plant macrofossils, which are partly decomposed plant material, are key to identifying past peat-forming vegetation (e.g. Barber *et al.*, 1998; Mauquoy *et al.*, 2002 a, b; Tuittila *et al.*, 2007; Väliiranta *et al.*, 2007), whereas pollen analysis, which calculates inputs of different pollen grains in peat sequence, can be applied as a complementary proxy to depict wider regional-scale changes in climate and associated vegetation shifts (e.g. Kaakinen and Eronen 2000).

Typically, bog peat layers which have not been affected by permafrost contain relatively well-preserved plant material for palaeoecological examination (Väliiranta *et al.*, 2007), whereas fen peat and peat found in deep permafrost layers is often highly humified (Lamarre *et al.* 2012; Oksanen *et al.* 2001), which in turn constrains the identification of plant remains (e.g. Moore *et al.*, 2007; Strakova *et al.* 2011) and historical habitat reconstructions. Thus,

1
2
3
4
5
6
7
8
9
10
11
12
13
14
15
16
17
18
19
20
21
22
23
24
25
26
27
28
29
30
31
32
33
34
35
36
37
38
39
40
41
42
43
44
45
46
47
48
49
50
51
52
53
54
55
56
57
58
59
60

there is a need to identify new methods that can be applied to study these problematic highly humified layers more accurately, preferably in combination with traditional palaeobotanical proxies. Recent studies of biomarkers in boreal peat environments, conducted both by solvent extraction of total lipids and the analysis of the non-extractable residues, have shown that plant group-specific chemical compounds can be applied to identify vegetation contributions to bog peat (e.g. Abbott *et al.* 2013; Avsejs *et al.*, 2002; Bingham *et al.*, 2010; Jia *et al.*, 2008; McClymont *et al.*, 2008; Ronkainen *et al.* 2014; Xie *et al.*, 2000). The most widely analyzed compounds have been the *n*-alkanes: for instance, the difference between concentrations of mid chain length (*n*-C₂₃ and *n*-C₂₅) and long chain length (*n*-C₂₉ to *n*-C₃₃) *n*-alkanes have been used to separate contributions of *Sphagnum* and vascular plant species in the peat (e.g. Andersson *et al.*, 2011; López-Días *et al.*, 2010; Ortiz *et al.*, 2011; Ronkainen *et al.*, 2013). However, studies focused on biomarker performance in highly humified fen peats are still scarce and accordingly it is difficult to assess the applicability of the biomarker method on highly humified peat (Andersson and Meyers 2012; Andersson *et al.*, 2011; Ronkainen *et al.* 2014). The existing palaeoecological fen studies have applied information on the chemical compounds derived from modern boreal or temperate bog plants (Routh *et al.*, 2014; Andersson and Meyers 2012; Andersson *et al.*, 2011). Only recently has information of the biomarker composition of fen plants been introduced (Huang *et al.*, 2011; Ronkainen *et al.*, 2013), and so far information on arctic plants is still lacking. Here, we search for supplementary proxies to investigate highly humified peat that is typical to permafrost environments (e.g. Andersson *et al.*, 2011; Oksanen *et al.*, 2001; Välranta *et al.*, 2003).

Permafrost peatlands are important for the global carbon cycle, as they are estimated to store *ca.* 40% of the global soil C pool (Tarnocai *et al.*, 2009). Recently their role within the global nitrogen cycle is increasingly discussed, since high N₂O emissions associated with permafrost melting (Elberling *et al.*, 2010) and frost-action (Marushchak *et al.*, 2011; Repo *et al.*, 2009)

were discovered. Frost action, which causes cracking of the soil surface, often creates and maintains a unique surface pattern characterized by un-vegetated bare peat circles on permafrost peatlands (Bockheim and Tarnocai 1998; Seppälä 2003). Unlike the surrounding vegetated surfaces, these un-vegetated peat circles have received attention as sources of relatively high emissions of the greenhouse gas N_2O as stated above (Repo *et al.* 2009), which is the third largest greenhouse gas contributor to positive radiative forcing after CO_2 and CH_4 (IPPC 2013). The hemispheric distribution of these bare peat circles is not homogenous, but where they do occur they can be regionally quite abundant with up to 50% coverage of the land surface (Repo *et al.* 2009) (Fig. 1). The formation of the un-vegetated surfaces has vaguely been linked to cryoturbation (Repo *et al.* 2009) but real understanding of the mechanisms requires further examination of their development history. To address this issue the best possible proxy combination is needed.

In the present study, as a part of a larger project examining past, present and future C and N dynamics of permafrost peatlands characterized by un-vegetated peat circles, we aim to combine palaeobotanical (macrofossils and pollen), biogeochemical and chronological analyses to one permafrost peat core to evaluate the suitability of the biomarker method to the permafrost environments. We first assess the biomarker composition of the common peatland plants in the arctic to create a local reference training data set of plant biomarkers. The new training set will be evaluated against previous work to test whether northern peatlands have a “universal” plant biomarker distribution.

2. Material and methods

2.1. Study site and sampling

1
2
3
4
5
6
7
8
9
10
11
12
13
14
15
16
17
18
19
20
21
22
23
24
25
26
27
28
29
30
31
32
33
34
35
36
37
38
39
40
41
42
43
44
45
46
47
48
49
50
51
52
53
54
55
56
57
58
59
60

95 The studied peat plateau is located in the discontinuous permafrost zone in the arctic East
96 European Russian tundra (67°03'N, 62°57'E, Komi Republic) (Fig 1), at a study site called
97 Seida, which is located near Vorkuta city. The peat plateau is elevated a few meters from the
98 surrounding mineral soil, and the highest parts are characterized by dwarf shrubs such as
99 *Betula nana*, *Rhododendron tomentosum* (syn. *Ledum palustre*), *Rubus chamaemorus*, and
100 hummock mosses *Sphagnum fuscum*, *Polytrichum strictum* and *Dicranum elongatum*.
101 Sedges, such as *Carex aguaticilis* and *Eriophorum* sp., and lawn mosses such as *Sphagnum*
102 *lindbergii* dominate lower and wetter surfaces. We collected a 1.6-m-long peat sequence from
103 a bare peat surface in summer 2012. The permafrost-free active peat layer (40 cm) was
104 sampled with a Russian peat corer and the underlying permafrost peat with a motorized corer.
105 The core was cut into 2-cm sample slices. Palaeobotanical, biogeochemical and chronological
106 analyses were conducted with varying resolution from the same samples throughout the
107 sequence. To study the biomarker composition of the most common peatland plants, we
108 collected and analyzed the total neutral lipid fractions of 13 most representative tundra peat
109 plateau plants collected from the vicinity of the coring point (Supplementary information
110 Table 1).

111

112 2.2. Plant macrofossil analyses

113 Samples with a volume of 5 cm³ were rinsed under running water using a 140-µm sieve,
114 without any chemical treatment. Remains retained on a sieve were identified and proportions
115 of different plant remains were visually estimated using a stereomicroscope (magnification of
116 10x) (e.g. Speranza *et al.*, 2000; Mauquoy *et al.*, 2002a; 2002b). More specific species
117 identification was done using a high power light-microscope (cf. Väliranta *et al.* 2007). In

1
2
3 118 addition to identifiable plant remains, the proportion of unidentified organic matter (UOM)
4
5 119 was estimated.
6
7
8
9 120

10
11
12 121 *2.3. Pollen analysis*
13
14

15 122 Pollen samples were prepared using standard methods described by Bennett and Willis
16
17 123 (2001). A minimum of 1000 pollen grains and spores of terrestrial vascular plants were
18
19 124 counted from each sample, using a light microscope with 400× magnification. After the sum
20
21 125 of 1000 was reached, the counting was continued with only new pollen taxa recorded,
22
23 126 together with grains of a reference taxon (*Picea abies*), to calculate percentage values for any
24
25 127 new taxa found. Pollen taxonomy follows Bennett (2004) modified for Sweden using the
26
27 128 checklist by Karlsson (1997).
28
29
30
31
32 129

33
34
35 130 *2.4. Radiocarbon dating*
36
37

38 131 Six bulk peat samples were ¹⁴C dated in Poznań Radiocarbon Laboratory Poland. ¹⁴C dates
39
40 132 were calibrated in the CALIB software (Stuiver and Reimer 1993) version 7.0.0, using the
41
42 133 IntCal13 calibration curve (Reimer *et al.* 2013). An age-depth model was calculated using the
43
44 134 method of Heegaard *et al.* (2005) in R (version 2.15.0) (R Development Core Team 2012).
45
46
47
48
49 135

50
51
52 136 *2.5. Solvent extraction*
53
54

55 137 Fresh plant and peat samples for solvent extraction were freeze dried and ground to
56
57 138 homogenous mass following the same procedure as in Ronkainen *et al.* (2013). For lipid
58
59
60

1
2
3
4
5
6
7
8
9
10
11
12
13
14
15
16
17
18
19
20
21
22
23
24
25
26
27
28
29
30
31
32
33
34
35
36
37
38
39
40
41
42
43
44
45
46
47
48
49
50
51
52
53
54
55
56
57
58
59
60

139 extraction of the samples ca. 0.2 g of sample was ultrasonicated for 20 min with 6 ml
140 CH₂Cl₂/MeOH (3:1, v/v). Saponification of samples was conducted by adding 0.5 M
141 methanolic (95%) NaOH and by heating the samples for 2 h at 70 °C. The neutral lipids were
142 extracted using hexane. Activated Al₂O₃ columns were used to separate the neutral lipids into
143 apolar and polar compounds, by eluting with hexane/CH₂Cl₂ (9:1, v/v) and CH₂Cl₂/MeOH
144 (1:2, v/v), respectively. Prior to gas chromatography (GC) and GC-mass spectrometry (GC-
145 MS) analysis the polar fraction of the samples were derivatised using
146 bis(trimethylsilyl)trifluoroacetamide (Sigma Aldrich).

147

148 2.6. GC-MS

149 Apolar and polar fractions were analyzed using GC-MS with the gas chromatograph
150 equipped with split/splitless injection (280 °C). Separation was achieved with a fused silica
151 column (30 m x 0.25 mm i.d) coated with 0.25µm 5% phenyl methyl siloxane (HP-5MS),
152 with He as carrier gas, and the following oven temperature program: 60 – 200 °C at 20
153 °C/min, then to 320 °C (held 35 min) at 6°C/min. The mass spectrometer was operated in full
154 scan mode (50-650 amu/s, electron voltage 70 eV, source temperature 230 °C). Compounds
155 were assigned using the NIST mass spectral database and comparison with published spectra
156 (e.g. Goad and Akihisa, 1997; Killops and Frewin, 1994). Quantification was achieved
157 through comparison of integrated peak areas in the FID chromatograms and those of internal
158 standards of known concentration (5-α-cholestane for apolars, 2-nonadecanone for polars).
159 Biomarker concentrations were normalized to total organic carbon (TOC) content and are
160 presented here as concentration per g TOC, so that samples with different extent of
161 degradation become comparable (Meyers 2003; Ortiz *et al.*, 2010).

1
2
3 162 Total organic C and N were measured by LECO TruSpec Micro CHNS-analyzer (Leco
4
5 163 Corporation, Michigan USA) from *c.* 2 mg dried and ground samples. In a three phase
6
7 164 analysis cycle the sample is first combusted in furnace with 1075 °C and with He as a carrier
8
9 165 gas flushed to the secondary oven (850 °C) for reduction and further particulate removal. In
10
11 166 the analyses phase the combustion gases pass the infrared detectors for CHS-measurements
12
13 167 and Lecosorb/Anhydrone -tubes for CO₂ and H₂O removal. After that C and N are measured
14
15 168 by thermal conductivity detector and results are computed as concentrations from the detector
16
17 169 signal.
18
19
20
21
22 170
23
24

25 171 2.7. Statistical analyses

26
27

28 172 We applied principal component analysis (PCA) to study the variation of biomarkers within
29
30 173 the studied fresh plant samples. In the first PCA we included all the identified compound
31
32 174 groups: sterols, *n*-alcohols (C₂₀-C₃₀), triterpenoids and *n*-alkanes (C₂₀-C₃₅) (µg/g TOC) and *n*-
33
34 175 alkane ratios. After that we used PCA to study the variation in the compound groups
35
36 176 separately to compare how well they were able to separate the plant species. Prior to all the
37
38 177 ordination analyses the biomarker data was log transformed and centered and standardized.
39
40
41

42 178 To relate the macrofossil and biomarker composition in the peat sequence we first clustered
43
44 179 depth groups that share similar abundance peaks of macrofossils in the studied peat sequence
45
46 180 using Two Way Indicator SPecies ANalysis (Twinspan for Windows 2.3). Prior to the
47
48 181 analysis the abundances of macrofossils were standardised from 0 to 1 by setting the highest
49
50 182 abundance of each unit to 1 and calculating other values as a percentage of the highest
51
52 183 abundance of the unit. In the analysis we used five cut levels (0.0, 0.2, 0.4, 0.6 and 0.8) of
53
54 184 macrofossil abundances and two division levels, which determines the maximum level of
55
56
57
58
59
60

1
2
3
4
5
6
7
8
9
10
11
12
13
14
15
16
17
18
19
20
21
22
23
24
25
26
27
28
29
30
31
32
33
34
35
36
37
38
39
40
41
42
43
44
45
46
47
48
49
50
51
52
53
54
55
56
57
58
59
60

185 recursive splitting for samples (Hill and Šmilauer 2005). Also, a PCA was conducted to
186 inspect if the variation in peat biomarker data (sterols, *n*-alcohols (C₂₀-C₂₈), triterpenoids and
187 *n*-alkanes (C₂₀-C₃₅) (µg/g TOC), and *n*-alkane ratios) relates to variation in plant macrofossil
188 data. We applied depth groups defined by TWINSpan as nominal supplementary variables
189 to determinate whether the peat biomarkers show specific compounds for the depth groups
190 constituted by the macrofossil. Similar PCA was also conducted to *n*-alkane ratios to find 10
191 best explaining ratios in the peat sequence. Multivariate analyses were conducted by using
192 Canoco for Windows 4.52 (ter Braak and Smilauer 2002).

193

194 **3. Results**

195 *3.1. Biomarker composition of the living tundra plants*

196 The apolar fractions of the tundra plants were dominated by homologous series of *n*-alkanes,
197 with minor contributions from other lipids e.g. squalene. Mixed samples of different lichen
198 species which presently dominate peat plateaus were characterized by the domination of the
199 C₃₁ *n*-alkane together with *n*-C₂₉ (Supplementary information Table 1). A moss species
200 *Dicranum elongatum* was also dominated by *n*-C₃₁, while *Sphagnum* mosses were dominated
201 by mid chain length alkanes *n*-C₂₅ (in *S. fuscum*) and *n*-C₂₃ (in *S. balticum* and *S. lindbergii*).
202 The *n*-alkane concentrations in shrub leaves, except in *V. uliginossum*, were substantially
203 higher (> 500 µg gTOC) than in mosses, lichens and shrub roots. In *L. palustre* and *E.*
204 *nigrum* leaves *n*-C₃₁ was the dominating *n*-alkane, and in *B. nana* and *V. uliginossum* leaves
205 *n*-C₂₇ dominated. Roots of *B. nana*, *L. palustris*, *E. nigrum* were dominated by *n*-C₂₉ and for
206 *V. uliginossum* roots by *n*-C₂₈. Both the leaves and roots of *R. chameamorus* were dominated
207 by *n*-C₂₇ with clearly lower concentration compared to other leaves. Long chain *n*-alkanes
208 dominated in all studied sedges: *n*-C₂₇ in *C. aquatilis* leaves and roots, *n*-C₂₉ in *Eriophorum*

209 sp. leaves and $n\text{-C}_{27}$ in *Eriophorum* sp. roots. *Betula pubescens* ssp. *czerepanovii*, syn.
210 *Tortuosa* leaves, bark and wood matter were dominated by long-chain $n\text{-C}_{27}$. *B. pubescens*
211 leaves clearly had the highest concentration of n -alkanes ($n\text{-C}_{27}$ ca. 2500 $\mu\text{g TOCg}$) when
212 compared to all studied plants (Supplementary information Table 1). Several n -alkane ratios
213 have previously been proposed as means of distinguishing different inputs to peatlands. We
214 tested these ratios for our new analyses of tundra plants, and confirm that some of the n -
215 alkane ratios are able to separate *Sphagnum* mosses from the rest of the plants. Particularly
216 effective were the ratios $n\text{-C}_{23}/n\text{-C}_{27}$, $n\text{-C}_{25}/n\text{-C}_{29}$, and $n\text{-C}_{23}/(n\text{-C}_{23}/n\text{-C}_{29})$. *B. nana* and
217 *pubescens* leaves could be separated from the rest of the plants by high values of the ratio $n\text{-C}_{23}/n\text{-C}_{21}$. High values of the $n\text{-C}_{25}/n\text{-C}_{21}$ ratio separated *V. uliginossum* and both *Betula*
218 species leaves from rest of the samples. Squalene was found from all studied vascular plant
219 samples but not in mosses or lichens. Squalene was most abundant in *R. chamaemorus*
220 leaves, and the roots of evergreen plants roots (*E. nigrum*, *V. uliginossum*, *L. palustre*).
221 Triterpenoids, such as taraxer-14-ene or taraxast-20-ene, were not detected in the samples
222 (Supplementary information Table 1).

224 The polar fraction of the sampled plants gave mixed results. The dominating n -alcohol and its
225 concentration varied in samples without any clear pattern between mosses, vascular plant
226 roots or leaves. Phytol [(3,7,11,15-tetramethylhexadec-2-en-1-ol)] was found in all other
227 samples excluding the roots. The concentrations were highest in *R. chamaemorus* leaves and
228 in *S. lindbergii*. Brassicasterol [(22 E)-ergosta-5,22-dien-3 β -ol] was found with greatest
229 concentration in lichen sp., and it was only additionally detected in *D. elongatum*, *S. fuscum*,
230 *S. balticum* and leaves of *E. nigrum*. Campesterol [campest-5-en-3 β -ol] and stigmasterol
231 [(24 E)-stigmasta-5,22-dien-3 β -ol] were found in a wider range of samples, but the
232 concentrations were highest in *Sphagnum* mosses, *D. elongatum* and lichen spp. All samples
233 contained β -sitosterol [(3 β)-stigmast-5-en-3-ol], and the highest concentrations were found

1
2
3
4
5
6
7
8
9
10
11
12
13
14
15
16
17
18
19
20
21
22
23
24
25
26
27
28
29
30
31
32
33
34
35
36
37
38
39
40
41
42
43
44
45
46
47
48
49
50
51
52
53
54
55
56
57
58
59
60

234 from *B. pubescens* wood matter, *R. chamaemorus* leaves and *L. palustre* roots
235 (Supplementary information Table 1). The polar fraction of *E. nigrum*, *V. uliginossum* and *B.*
236 *nana* root samples were omitted from the analyses as the samples were contaminated and
237 reliable results were not received.

238

239 3.2. Multivariate analyses of the biomarker distribution in the living tundra plants

240 PCA with all identified biomarkers separated the three groups: mosses, vascular plant roots
241 and leaves along the first two axes explaining 52% of the variation (1st 30% and 2nd 22%).
242 The concentration of most of the biomarkers showed an increasing trend towards the vascular
243 plant leaves, with only high C₂₀ *n*-alkane concentrations and a high ratio of *n*-C₂₁/*n*-C₂₃
244 together with high campesterol and stigmasterol concentrations being typical for *Sphagnum*
245 mosses. Lichens, *D. elongatum*, *B. pubescens* wood matter and bark grouped together with
246 vascular plant roots (Fig 2).

247 Biomarker compound groups analyzed separately differed in their ability to separate plants.
248 In the PCA with *n*-alkane concentrations, the first axis already explained 51% of the
249 variation (Supplementary information Figure 1) and separated *E. nigrum*, *L. palustre* and *B.*
250 *pubescens* from the rest of the sampled plants. *E. nigrum* and *L. palustre* showed high
251 concentrations of *n*-alkanes *n*-C₂₉, *n*-C₃₀, *n*-C₃₁, *n*-C₃₂ and *n*-C₃₃, and *B. pubescens* leaves
252 have high concentration of *n*-alkanes *n*-C₂₃, *n*-C₂₄, *n*-C₂₅ and *n*-C₂₆. In the PCA with *n*-
253 alkanes ratios, the first axis explained 58% of the variation and separated clearly the
254 *Sphagnum* mosses, and *B. nana* and *pubescens* to their own groups (Supplementary
255 information Figure 1). In the PCA with the *n*-alcohols the first axis explained 54% of the
256 variation. Analysis clearly separated the leaves of *B. nana* by *n*-C₂₁-ol and *n*-C₂₃-ol and *R.*

1
2
3 257 *chamaemorus* by *n*-C₂₉-ol from the rest of the sampled plants. Leaves of *B. pubescens*, *L.*
4
5 258 *palustre*, *V. uliginossum* and *C. aquatilis* were separated from mosses, lichens and roots
6
7 259 along the first axis, as the concentration of *n*-alcohols increased towards the leaves (Fig 4 d).
8
9
10 260 The PCA with plant sterols and triterpenoids grouped vascular plant leaves, roots and mosses
11
12 261 as separate clusters and the first axis explained 56% of the variation within the samples. High
13
14 262 concentrations of squalene and β -sitosterol described the leaves, low concentrations of phytol
15
16 263 described the roots and brassicasterol, campesterol and stigmasterol described *S. fuscum*, *S.*
17
18 264 *balticum*, *D. elongatum* and lichens (Supplementary information Figure 1).
19
20
21
22 265

23 24 25 266 3.3. Peat sequence chronology and deposition dynamics 26 27

28
29 267 The radiocarbon dates reveal that the studied peat sequence does not cover the whole
30
31 268 Holocene, and the top peat layer yielded an age 5900 cal a BP. The loss of the top part of the
32
33 269 sequence is likely due to erosion due to permafrost initiation and associated ground uplift.
34
35 270 Thus the studied peat sequence covers a time span 8400-5900 cal a BP (Table 1 and Fig 3).
36
37 271 The stratification of the peat sequence shows that directly after the peat initiation, ca. 8400
38
39 272 cal a BP, peat deposition was very fast, nearly 1 m during the first ca. 1000 years (i.e. 1 mm
40
41 273 a⁻¹). After 7400 cal a BP, the deposition rate slows down, to ca. 0.4 mm a⁻¹(Fig 3), which is
42
43 274 still relatively fast rate compared to rates reported in previous studies; ca. 0.2 mm a⁻¹ (e.g.
44
45 275 Oksanen *et al.* 2001; Botch *et al.* 1995).
46
47
48
49
50 276

51 52 53 277 3.4. Plant macrofossil composition of the peat sequence 54 55 56 57 58 59 60

1
2
3
4
5
6
7
8
9
10
11
12
13
14
15
16
17
18
19
20
21
22
23
24
25
26
27
28
29
30
31
32
33
34
35
36
37
38
39
40
41
42
43
44
45
46
47
48
49
50
51
52
53
54
55
56
57
58
59
60

278 Due to the lack of the top layer the palaeobotanical composition of the whole peat core
279 differed from the current vegetation. The palaeobotanical composition of the deepest peat
280 sequence that contained minerotrophic bryophytes and other fen species typical of nutrient-
281 rich conditions, such as *Filipendula ulmaria* and *Menyanthes trifoliata*, clearly indicated that
282 until ca. 6200 cal a BP the study site was a permafrost free minerotrophic site (Fig 3).
283 Moreover, abundant tree birch and spruce remains alongside a high number of seeds of *Carex*
284 and *Filipendula* suggest that at first, between ca. 8300 and 7500 cal a BP, the site was a
285 swamp or forested nutrient rich fen (zone I). After 7500 cal a BP the site became dominated
286 by sedges and *Menyanthes* and the habitat changed to oligotrophic open fen (zone II).
287 Vegetation composition changed abruptly ca. 6100 cal a BP. Between 6100 and 5900 cal a
288 BP (the core top) very few identifiable plant remains were detected, although at the very
289 surface some species that indicate dry bog conditions, such as *Empetrum nigrum* and
290 *Dicranum* sp. were found (zone III). The amount of UOM was relatively high throughout the
291 sequence suggesting a high level of decomposition. As an exception between ca. 7400 and
292 7200 cal a BP the peat was less decomposed and the amount of UOM was smaller
293 accompanied by a high amount of sedge remains.

294

295 3.5. Pollen stratigraphy

296 *Betula* sp., *Picea* and *Cyperaceae* appeared to be the dominant pollen taxa throughout the
297 sequence, typically together constituting 80–90% of all pollen (Fig 4). In addition, *Equisetum*
298 and *Filipendula* reach very high values of 50–60% in single samples. These peaks likely
299 represent highly localized, massive spore/pollen input, and coincide with abundant
300 occurrences of *Equisetum* vegetative remains and *F. ulmaria* seeds in the macrofossil record.

301

302 *3.6. Peat biomarkers*

303 Most of the peat samples were dominated by *n*-alkanes *n*-C₂₇ or *n*-C₂₉ suggesting domination
304 of vascular plant inputs (Supplementary Information Table 2). Exceptions to this dominance
305 occurred at depths 12 cm (dominance of *n*-C₂₃), 36 cm (equally dominant *n*-C₂₃, *n*-C₂₅ and *n*-
306 C₂₉), 56cm (*n*-C₂₅ and *n*-C₂₁), 64cm (*n*-C₂₁, *n*-C₂₃ and *n*-C₂₅), and 72 cm (*n*-C₂₃ and *n*-C₂₇). At
307 depths 56, 64 and 72 cm the overall concentrations of *n*-alkanes were also much lower than in
308 the rest of the analyzed core depths (Supplementary information Table 2). Variations in the *n*-
309 alkane ratios are also identified through the peat sequence. There was little variation in the
310 ratios between 166 and 80 cm, then between 70 to 50 cm most of the ratios increased in
311 value, before fluctuating and decreasing towards the core top (through 50 – 0 cm,
312 Supplementary information Figure 2). Taraxer-14-ene was found only from the very top
313 layers of the peat core, and similarly urs-20-ene was not found from the bottom layers but
314 only above 104 cm. In contrast, taraxast-20-ene was detected throughout the peat sequence
315 and showed two prominent peaks at 112 and 44 cm (Supplementary information Table 2).

316 In the polar fraction of the peat sequence two samples, 4 and 88 cm, and the values of *n*-C₂₂-
317 ol from all of the samples were omitted due to contamination. The *n*-alcohols formed three
318 zones according to the dominating compounds: between 166 and 52 cm C₂₈-ol dominated
319 most of the layers, between 144 and 128 cm *n*-C₂₆-ol dominated, at 64 cm *n*-C₂₃-ol
320 dominated, between 48 – 32 cm there was varied domination by *n*-C₂₄-ol, *n*-C₂₆-ol and *n*-C₂₈-
321 ol, and between 24 and 0 cm *n*-C₂₄-ol mainly dominated. β -sitosterol and the related 3-
322 stigmastanol [(24-ethyl-5 α -cholestan-3 β -ol)] were present throughout the sequence, the
323 highest concentration of β -sitosterol was detected from the sample 52 cm (14 000 μ g TOCg),
324 but overall there was no clear trend through the sequence. Campesterol and the related

1
2
3
4
5
6
7
8
9
10
11
12
13
14
15
16
17
18
19
20
21
22
23
24
25
26
27
28
29
30
31
32
33
34
35
36
37
38
39
40
41
42
43
44
45
46
47
48
49
50
51
52
53
54
55
56
57
58
59
60

campestanol [24-methyl-5 α -cholestan-3 β -ol] were found from sample depths 72 – 0 cm, and the campesterol concentration was highest at 0 cm (1400 μ g TOCg). Stigmasterol and the related 22E-stigmastanol [(24-ethyl-5 α -cholest-22-3 β -ol)] were found only from the very top layers of the sequence (Supplementary information Table 2).

3.7. Plant macrofossil and biomarker distribution in the peat sequence

Based on the identified macrofossils TWINSpan divided the studied peat sequence into three depth groups (Table 2). The first group (bog, zone III) included only the top peat sample with bog plant macrofossils. The second (swamp, zone I) and third (open fen, zone II) groups divided the fen peat sequence to peat layers with high presence of woody and other drier habitat plant macrofossils, and layers dominated by sedge and *M. trifoliata* remains as indicators of wetter habitat, respectively. When we applied the three depth groups, bog, swamp and fen, determined by the macrofossil TWINSpan as supplementary environmental variables to a PCA for biomarkers, some depth group specific biomarkers could be pointed out in figure 5. The bog group (0cm) stands out from the other two but no specific compound described it. Depths and related biomarkers of swamp fen group was separated most clearly and described by *n*-C₃₄, *n*-C₃₅, ratio *n*-C₃₁/ *n*-C₂₇, taraxast-20-ene and phytol . In contrast, the depths and biomarkers of the fen group were situated with a wide range in the ordination space characterized by a high number of different compounds.

3.8. Degradation measures

1
2
3 346 In studying a peatland core and making comparisons to modern living plants, it is important
4
5 347 to recognize that organic matter degradation may alter or mask the original signals produced
6
7 348 in the plants. Consequently biomarkers may not fully reflect the organic matter sources and
8
9
10 349 its preservation in peat (Zheng *et al.* 2007). Bulk density (g/cm^3), C/N ratio, and the
11
12 350 proportion of C were all relatively stable throughout the peat sequence (Fig 3, Supplementary
13
14 351 information Table 2). The ratio of 3-stigmastanol/ β -sitosterol (Andersson and Myers, 2012),
15
16 352 which indicates the microbially mediated degradation of sterols similarly to the $5\alpha(\text{H})$ -
17
18 353 stanols/ Δ^5 -sterol ratio, stayed stable (0.3 – 0.5) through the sequence, except at depths 150,
19
20 354 52, 8 and 0 cm where the ratio was slightly lower, ca. 0.2. The carbon preference index (CPI:
21
22 355 cf. Andersson and Meyers 2012), where high values are associated with well-preserved
23
24 356 organic material (e.g. Andersson and Meyers 2012), showed some variation in the sequence,
25
26 357 but the low values throughout the sequence in general suggest a high level of organic matter
27
28 358 degradation (Supplementary information Table 2).
29
30
31
32
33 359

360 4. Discussion

361 4.1. Biomarkers of sub-arctic peat plateau plants

362 Previous studies on modern plant biomarker compositions from peatlands have concentrated
363 on boreal and north temperate areas of Europe, excluding a recent study conducted in
364 extreme-continental Asia (Tarasov *et al.*, 2013), whereas so far data from arctic locations has
365 been lacking. Our results show that the total lipid fractions of the studied subarctic peat
366 plateau plants are similar to plants from more southern locations: lichens are dominated by *n*-
367 C_{31} alkane (Ficken *et al.*, 1998; Nott *et al.*, 2000), *Sphagnum* mosses by *n*- C_{25} (*Sp. fuscum*)
368 and *n*- C_{23} (*Sp. balticum* and *S. lindbergii*) (e.g. Ficken *et al.*, 1998; Baas *et al.*, 2000;

1
2
3
4
5
6
7
8
9
10
11
12
13
14
15
16
17
18
19
20
21
22
23
24
25
26
27
28
29
30
31
32
33
34
35
36
37
38
39
40
41
42
43
44
45
46
47
48
49
50
51
52
53
54
55
56
57
58
59
60

Bingham *et al.*, 2010), *C. aquatilis* leaves by $n\text{-C}_{27}$ (Ficken *et al.*, 1998; Ficken *et al.*, 2000; Ronkainen *et al.*, 2013) and roots by $n\text{-C}_{27}$, *Eriophorum* sp. leaves by $n\text{-C}_{29}$ (Nott *et al.*, 2000) and roots by $n\text{-C}_{27}$ (Ronkainen *et al.*, 2013). Dwarf shrubs also showed similar compositions as the previous studies (Salasoo 1987; Ficken *et al.*, 1998; Nott *et al.*, 2000; Tarasov *et al.*, 2013). Birch leaves, bark and wood were dominated by $n\text{-C}_{27}$ corresponding to results reported by Sachse *et al.* (2006) and Tarasov *et al.* (2013). When the biomarker distributions of studied plants were analyzed with PCA, the n -alkanes, their ratios, and the sterols and triterpenoids explained the differences best, whereas n -alcohols were not effective as we previously observed in boreal fen plants in Finland (Ronkainen *et al.*, 2013). The long chain length n -alkanes $n\text{-C}_{29}$ to $n\text{-C}_{33}$ were characteristic for evergreen shrub leaves and the mid chain length n -alkanes $n\text{-C}_{23}$ to $n\text{-C}_{26}$ described *B. pubescens* leaves rather than *Sphagnum* mosses. The reason for this pattern is the much higher total concentration of n -alkanes in *B. pubescens* leaves when compared to *Sphagnum* mosses. The n -alkane ratios such as $n\text{-C}_{25}/n\text{-C}_{29}$, $n\text{-C}_{23}/n\text{-C}_{27}$, $n\text{-C}_{23}/(n\text{-C}_{27} + n\text{-C}_{31})$ and P_{wax} separated *Sphagnum* mosses from vascular plants, while the ratio $n\text{-C}_{23}/n\text{-C}_{21}$ had distinguishably high values for both *B. pubescens* and *nana* leaves. The presence of campesterol, brassicasterol and stigmasterol were indicative for mosses and lichens, while high amount of β -sitosterol and squalene was typical for vascular plant leaves, as suggested by Ronkainen *et al.* (2013) for boreal fen species. Our results imply that if the plant biomarker data is generally valid any established modern biomarker training-set of peatland plants could be universally applied to palaeoecological studies on peat archives.

4.2. Permafrost peat stratigraphy - proxy comparison

1
2
3 392 The radiocarbon and macrofossil data indicate consistent chronology and a succession from a
4
5 393 swamp (nutrient rich forested fen) (zone I: 166-82 cm) towards a wetter and nutrient poorer
6
7 394 open fen environment dominated by sedges (zone II: 72-8 cm) and ultimately to dry
8
9 395 ombrotrophic bog (zone III: 4-0 cm). Statistical inspection of the macrofossil data confirmed
10
11 396 the zonal division of the sequence (Table 2 and Fig 3). During 8400 - 6000 cal a BP the site
12
13 397 remained permafrost free (Fig 3). The pollen data provides supportive evidence of unchanged
14
15 398 vegetation and environmental conditions (Fig 4): although the macroscopic tree remains were
16
17 399 not found in the record during that time period, the pollen assemblages did not change. This
18
19 400 pollen record suggests that spruce and birch were present and there was no regional-scale
20
21 401 environmental change as could be interpreted based only on the macrofossil record. Due to
22
23 402 loss of the uppermost peat layer we lack the part of the deposition history that contains
24
25 403 permafrost initiation.
26
27
28
29

30
31 404 The PCA with peat biomarkers and depth groups derived from macrofossil distribution was
32
33 405 able to point out some peatland phase-related markers for the swamp phase (zone I): $n\text{-C}_{34}$, $n\text{-C}_{35}$,
34
35 406 taraxast-20-ene, and for the open fen phase (zone II): a wide range of n -alkanes and n -
36
37 407 alcohols, β -sitosterol and stanols. Bog (zone III) was separated as its own group but no
38
39 408 specific biomarkers described it (Table 2, Fig 5). Interestingly, when compared to the n -
40
41 409 alkane ratio compositions of the living plants, the PCA for peat (Supplementary information
42
43 410 Figure 1) suggests the presence of *Sphagnum* mosses in the fen phase (e.g. $n\text{-C}_{25}/n\text{-C}_{29}$, $n\text{-C}_{25}/$
44
45 411 $(n\text{-C}_{25} + n\text{-C}_{29})$, in zone II) an important plant group forming biomass in oligotrophic
46
47 412 fens (Laine *et al.*, 2012), while the macrofossil record showed predominance of sedges and
48
49 413 *Equisetum* (Fig 3). The n -alkane ratios of the peat sequence (Fig 6) also indicate a possible
50
51 414 presence of *Sphagnum* mosses in the fen phase. This suggests that biomarkers do have
52
53 415 potential to show occurrence of plants not seen in the traditional methods but also that several
54
55 416 biomarker groups should be concurrently involved. A failure to detect *Sphagnum* occurrence
56
57
58
59
60

1
2
3
4
5
6
7
8
9
10
11
12
13
14
15
16
17
18
19
20
21
22
23
24
25
26
27
28
29
30
31
32
33
34
35
36
37
38
39
40
41
42
43
44
45
46
47
48
49
50
51
52
53
54
55
56
57
58
59
60

would act as a serious flaw for reconstruction of past C and N dynamics. The overall trend in the PCA was an increase of the number and concentration of the detected biomarkers towards the surface peat layers, which could indicate higher decomposition rate in the deeper peat layers resulting in lower lipid concentrations overall. In open fen layers (zone II), the higher P_{aq} ($[n-C_{23}+n-C_{25}) / (n-C_{23}+n-C_{25}+n-C_{29}+n-C_{31}]$; Ficken *et al.* 2000) values (0.6-0.7) are consistent with development of a wet fen phase in the sequence, an association also observed by Andersson *et al.* (2011) who reported similar values for wet fen phase in permafrost peat sequence. The alkane ratio $n-C_{23} / (n-C_{27} + n-C_{31})$ was also proposed by Andersson *et al.* (2011) to differentiate fen and bog habitats in subarctic peats, whereby ratios >0.2 would indicate bog peat and ratios <0.2 would indicate fen peat. In our study, the $n-C_{23} / (n-C_{27} + n-C_{31})$ ratio was not among those 23 biomarker signals that had a strong explanatory value (Fig 5). In our sequence this interpretation would suggest that swamp fen (III) and bog (I) zones both consist of bog peat, and that only the fen zone (II) is actually fen peat. Accordingly, this ratio succeeds to separate the wet open fen phase (zone II) but fails to identify the drier swamp phase (zone I) and it would rather work as an indicative marker for moisture changes than a peat type indicator, as sedges are the main component of swamp and open fen peat.

The macrofossil record suggests a change from open fen to bog environment at the top of the sequence. Although modern aeration and freeze-thaw activity is influencing the top layers, the low 3-stigmastanol/ β -sitostanol ratio and high CPI value at the top peat indicates less humified peat than in the deeper layers. However, it is possible that the sparse bog plant macrofossils in the very top layers represent modern plants that have invaded the site, i.e. they do not represent the plant assemblage of 5900 cal yr BP. This interpretation is supported by the biomarker record that showed no indications of a transition from fen to bog habitat in the top layers, such as changes in *n*-alkane domination from long to mid chain length, *n*-alkane, sterols or triterpenoids concentrations, or in the *n*-alkane ratios (cf. Ronkainen *et al.*

2014). The shift to C₂₇ *n*-alkane domination could be explained by the remains of deciduous leaves on the top layers, deposited to the surface from surrounding vegetation dominated by *B. nana* and *V. uliginossum*. Finally, the identified macrofossils on top of the peat sequence resemble the present overall dominating vegetation at the surrounding vegetated peat plateau.

In addition to the three vegetation zones both macrofossil and biomarker data showed a momentary change around 7500 – 7200 cal a BP (72 – 52 cm), which is also detected in the statistical data observation procedure which separated these depths due to association with squalene, into a sub-group within the open fen zone (Fig 5). The change is characterized by a simultaneous decrease in the amount of UOM and an increase in the amount of sedge and shrub root remains. Unlike Andersson *et al.* (2011) we did not detect a corresponding peak of C₃₁ *n*-alkane with abundant shrub rootlet remains; on the contrary, the total *n*-alkane concentration decreases and the dominance of the long chain length *n*-alkanes is replaced by a switch to mid chain length *n*-alkanes (Supplementary information Table 2). This pattern suggests that either *Sphagnum* mosses, *B. pubescens* leaves or sedge roots were present (Sachse *et al.* 2006; Ronkainen *et al.* 2013), while in the macrofossil record a small amount of sedge roots (light root matter) were present (Fig 3). Furthermore, most of the studied *n*-alkane ratios and concentrations of squalene, campesterol and β -sitosterol increased, indicating an increase in vascular plant input (Ronkainen *et al.* 2014), whereas the degradation measures, 3-stigmastanol/ β -sitostanol ratio and CPI value, stayed stable throughout the whole sequence (Supplementary information Table 2). The reduced *n*-alkane concentration therefore appears to be a sign of slower peat accumulation, rather than more effective degradation, as the 3-stigmastanol/ β -sitostanol ratio and CPI value did not show changes in degradation (Andersson and Meyers 2012; Ronkainen *et al.* 2014). The decreased amount of UOM together with relatively high amount of sedge remains supports the proposal of lower rate of accumulation rather than fast degradation, as sedge material is suggested in

1
2
3
4
5
6
7
8
9
10
11
12
13
14
15
16
17
18
19
20
21
22
23
24
25
26
27
28
29
30
31
32
33
34
35
36
37
38
39
40
41
42
43
44
45
46
47
48
49
50
51
52
53
54
55
56
57
58
59
60

467 general to be degraded fast due the litter quality and related microbial and enzyme activity
468 that is found in vascular plant litters (Bartsch and Moore 1985; Szumigalski and Bayley
469 1996; Strakova *et al.*, 2011).

470 The studied permafrost peat sequence was comprised mainly from highly humified fen peat
471 with no clear change to bog peat because it lacked the permafrost initiation event and
472 associated shift to true bog environment. A recent study by Routh *et al.* (2014) conducted at
473 same site on a vegetated peat plateau surface dated the permafrost initiation as late as ca. 2
474 200 cal a BP. Consequently, it can be hypothesized that either la great amount of organic
475 matter has been eroded by wind from surface of the study site or that the recent peat
476 accumulation has been extremely slow, or even some combination of these two assumed
477 mechanisms. To resolve this further studies are required including several well-dated peat
478 sequences from the same peatland. Despite the lost material the highly humified nature of the
479 peat and the large amount of UOM, the macrofossil data with support from the pollen record
480 succeeded to separate three different habitats from the studied sequence: swamp (zone I),
481 open oligotrophic fen (zone II) and bog (zone III). The biomarker record corresponded to
482 other proxy records: *n*-alkanes, *n*-alkane ratios, sterols and triterpenoids showed variation
483 along the sequence. The biomarker record indicated several shifts in moisture conditions (e.g.
484 P_{aq} and $n-C_{23} / (n-C_{27} + n-C_{31})$) along the sequence, and suggested that the higher plants were
485 dominating most of the time through the presence of long chain *n*-alkanes, and the high
486 concentrations of sterols and triterpenoids (Ronkainen *et al.* 2014). Some of the *n*-alkane
487 ratios (e.g. $n-C_{25}/n-C_{29}$ and $n-C_{23}/n-C_{27}$) in the fen phase might also indicate the presence of
488 *Sphagnum* mosses while the macrofossil evidence does not detect this (Supplementary
489 information Figure 2). Thus, even though similarities in the biomarker and macrofossil data
490 sets existed, overall the data indicate that in highly humified permafrost peat environments
491 the macrofossils continue to be the most competitive proxy to reconstruct changes in

492 vegetation and local environmental conditions. An important implication of our study is that
493 it shows the value of combining both macrofossil and biogeochemical data sets to understand
494 better the peatland evolution - as previously suggested in several other studies (e.g.
495 Andersson 2012; Ficken *et al.*, 1998; Pancost *et al.*, 2002; Ronkainen *et al.* 2014).

496

497 5. Conclusions

498 Our results indicate, similarly to a recent study from extreme-continental Asia (Tarasov *et al.*,
499 2013), that lipid biomarker distributions of the common peatland plants are not affected by
500 geographical location of the study site. If generally valid, consequently any established
501 modern biomarker training-set of peatland plants could be universally applied to
502 palaeoecological studies.

503 By applying combined biogeochemical, palaeobotanical and chronological methods we
504 discovered a consistent permafrost peatland development history. A combination of the
505 proxies indicated no clear transition in peat type from fen to bog peat and no signs of
506 cryoturbation were detected. The macrofossil analyses together with the chronology largely
507 provided the essential information about the development history of the site, while
508 biomarkers provided information about the top core peat resembling fen rather than bog peat
509 environment in contrast to the palaeobotanical proxy record. In addition the biomarkers
510 indicated, unlike macrofossils, a presence of *Sphagnum* mosses in the open fen stage. Thus, a
511 more robust reconstruction of the past peatland dynamics was best achieved by combining
512 palaeobotanical and biochemical data.

513

514

1
2
3
4
5
6
7
8
9
10
11
12
13
14
15
16
17
18
19
20
21
22
23
24
25
26
27
28
29
30
31
32
33
34
35
36
37
38
39
40
41
42
43
44
45
46
47
48
49
50
51
52
53
54
55
56
57
58
59
60

515 **Acknowledgements**

516 D. Kaverin and his students are acknowledged for their help in the sample coring. We thank
517 J. Menegazzo and M. West for the help in the laboratory, and J. Saren for conducting the
518 element analysis. T. Virtanen is acknowledged for producing the maps in Figure 1. Funding
519 from the Academy of Finland (codes 131409, 140863, 218101 and 201321) is acknowledged.

520

521 **References:**

522 Abbott GD, Swain EY, Muhammad AB, Allton K, Belyea LR, Laing CG, Cowie GL. 2013.
523 Effect of water-table fluctuations on the degradation of sphagnum phenols in surficial peats.
524 *Geochimica Et Cosmochimica Acta* **106**: 177-191.

525 Andersson R. 2012. Lipid biomarkers and other geochemical indicators in
526 paleoenvironmental studies of two Arctic systems, a Russian permafrost peatland and marine
527 sediments from Lomonosov Ridge. Doctoral thesis in Geochemistry, Stockholm University,
528 Sweden.

529 Andersson RA, Meyers PA. 2012. Effect of climate change on delivery and degradation of
530 lipid biomarkers in a Holocene peat sequence in the eastern European Russian arctic. *Organic*
531 *Geochemistry* **53**: 63-72.

532 Andersson RA, Kuhry P, Meyers P, Zebühr Y, Crill P, Mörtz M. 2011. Impacts of
533 paleohydrological changes on n-alkane biomarker compositions of a holocene peat sequence
534 in the eastern european russian arctic. *Organic Geochemistry* **42**: 1065-1075.

- 535 Avsejs LA, Nott CJ, Xie S, Maddy D, Chambers FM, Evershed RP. 2002. 5-*n*-
536 Alkylresorcinols as biomarkers of sedges in an ombrotrophic peat section. *Organic*
537 *Geochemistry* **33**: 861-867.
- 538 Baas M, Pancost R, Van Geel B and Sinninghe Damsté JS. 2000. A comparative study of
539 lipids in Sphagnum species. *Organic Geochemistry* **31**: 535-541.
- 540 Barber K, Dumayne-Peaty L, Hughes P, Mauquoy D, Scaife R. 1998. Replicability and
541 variability of the recent macrofossil and proxy-climate record from raised bogs: Field
542 stratigraphy and macrofossil data from Bolton fell moss and Walton moss, Cumbria,
543 England. *Journal of Quaternary Science* **13**: 515-528.
- 544 Bartsch I, Moore TR. 1985. A preliminary investigation of primary production and
545 decomposition in four peatlands near Schefferville, Quebec. *Canadian Journal of Botany* **63**:
546 1241-1248.
- 547 Bennett K, Willis K. 2001. Pollen. In: Tracking environmental change using lake sediments.
548 Terrestrial, algal, and siliceous indicators. Vol.3. Terrestrial, algal, and siliceous indicators.
549 Smol J.P., Birks H.J.B., Last W.M. edn. Dordrecht, The Netherlands: Kluwer Academic
550 Publishers
- 551 Bennett K. 2004. Pollen catalogue of the British Isles. ([http://chrono.qub.ac.uk/pollen/pc-](http://chrono.qub.ac.uk/pollen/pc-intro.html)
552 [intro.html](http://chrono.qub.ac.uk/pollen/pc-intro.html))
- 553 Bingham EM, McClymont EL, Väliranta M, Mauquoy D, Roberts Z, Chambers FM, *et al.*
554 2010. Conservative composition of n-alkane biomarkers in Sphagnum species: Implications
555 for palaeoclimate reconstruction in ombrotrophic peat bogs. *Organic Geochemistry* **41**: 214-
556 220.

1
2
3
4
5
6
7
8
9
10
11
12
13
14
15
16
17
18
19
20
21
22
23
24
25
26
27
28
29
30
31
32
33
34
35
36
37
38
39
40
41
42
43
44
45
46
47
48
49
50
51
52
53
54
55
56
57
58
59
60

557 Bockheim JG, Tarnocai C. 1998. Recognition of cryoturbation for classifying perma-frost-
558 affected soils. *Geoderma* **81**: 281–293.

559 Botch MS, Kobak KI, Vinson TS, Kolchugina TP. 1995. Carbon pools and accumulation in
560 peatlands of the former Soviet Union, *Global Biogeochemical Cycles* **9**: 37-46.

561 Elberling B, Christiansen HH, Hansen BU. 2010. High nitrous oxide production from
562 thawing permafrost. *Nature Geoscience* **3**: 332-335.

563 Ficken KJ, Barber KZ, Eglinton G. 1998. Lipid biomarker, δ 13C and plant macrofossil
564 stratigraphy of a Scottish montane peat bog over the last two millennia. *Organic*
565 *Geochemistry* **28**: 217-237.

566 Ficken KJ, Li B, Swain DL, Eglinton G. 2000. An *n*-alkane proxy for the sedimentary input
567 of submerged/floating freshwater aquatic macrophytes. *Organic Geochemistry* **31**: 745-749.

568 Goad LJ, Akihisa T. 1997. *Analysis of sterols*. Blackie Academic and Professional, Blackie
569 Academic and Professional, London.

570 Heegaard E, Birks HJB, Telford RJ. 2005. Relationships between calibrated ages and depth
571 in stratigraphical sequences: an estimation procedure by mixed-effect regression. *The*
572 *Holocene* **15**:612.618.

573 Hill MO, Šmilauer P. 2005. WinTWINS version 2.3. Available at
574 http://planet.uwc.ac.za/nisl/computing/Twinspace/userguide_twinspace.pdf (accessed 12
575 September 2013).

- 576 Huang X, Wang C, Zhang J, Wiesenberg GLB, Zhang Z, Xie S. 2011. Comparison of free
577 lipid compositions between roots and leaves of plants in the Dajiuhu Peatland, Central China.
578 *Geochemical Journal* **45**: 365-373.
- 579 IPCC, 2013: Climate Change 2013: The Physical Science Basis. Contribution of Working
580 Group I to the Fifth Assessment Report of the Intergovernmental Panel on Climate Change
581 [Stocker, T.F., D. Qin, G.-K. Plattner, M. Tignor, S.K. Allen, J. Boschung, A. Nauels, Y. Xia,
582 V. Bex and P.M. Midgley (eds.)]. Cambridge University Press, Cambridge, United Kingdom
583 and New York, NY, USA, 1535 pp.
- 584 Jia G, Dungait JAJ, Bingham EM, Väliranta M, Korhola A, Evershed RP. 2008. Neutral
585 monosaccharides as biomarker proxies for bog-forming plants for application to
586 palaeovegetation reconstruction in ombrotrophic peat deposits. *Organic Geochemistry* **39**:
587 1790-1799.
- 588 Kaakinen A, Eronen M. 2000. Holocene pollen stratigraphy indicating climatic and tree-line
589 changes derived from a peat section at ortino, in the pechora lowland, northern russia.
590 *Holocene* **10**: 611-620.
- 591 Karlsson T. 1997. Förteckning över svenska kärlväxter. The vascular plants of Sweden- a
592 checklist. *Svensk Botanisk Tidskrift* **91**: 241-560.
- 593 Killips SD, Frewin NL. 1994. Triterpenoid diagenesis and cuticular preservation. *Organic*
594 *Geochemistry* **21**: 1193-1209.
- 595 Laine A, Bubier J, Riutta T, Nilsson MB, Moore TR, Vasander H, Tuittila E-S. 2012.
596 Abundance and composition of plant biomass as potential controls for mire net ecosystem CO
597 2 exchange. *Botany* **90**: 63-74.

1
2
3 598 Lamarre A, Garneau M, Asnong H. 2012. Holocene paleohydrological reconstruction and
4
5 599 carbon accumulation of a permafrost peatland using testate amoeba and macrofossil analyses,
6
7 600 Kuujjuarapik, subarctic Quebec, Canada. *Review of palaeobotany and palynology*, **186** (SI):
8
9 601 131-141.
10
11
12 602 López-Días V, Borrego T, Blanco CG, Arboleya M, López-Sáez JA, López-Merino L. 2010.
13
14 603 Biomarkers in a peat deposit in Northern Spain (Huelga de Bayas, Asturias) as proxy for
15
16 604 climate variation. *Journal of Chromatography A* **1217**: 3538-3546.
17
18
19
20 605 Mauquoy D, Engelkes T, Groot MHM, Markesteijn F, Oudejans MG, Van Der Plicht J., *et al.*
21
22 606 a 2002. High-resolution records of late-Holocene climate change and carbon accumulation in
23
24 607 two north-west European ombrotrophic peat bogs. *Palaeogeography, Palaeoclimatology,*
25
26 608 *Palaeoecology* **186**: 275-310.
27
28
29
30 609 Mauquoy D, Van Geel B, Blaauw M, Van der Plicht J. b 2002. Evidence from northwest
31
32 610 European bogs shows 'Little Ice Age' climatic changes driven by variations in solar activity.
33
34 611 *Holocene* **12**: 1-6.
35
36
37
38 612 Marushchak ME, Pitkämäki A, Koponen H, Biasi C, Seppälä M, Martikainen PJ. 2011. Hot
39
40 613 spots for nitrous oxide emissions found in different types of permafrost peatlands. *Global*
41
42 614 *Change Biology* **17**: 2601-2614.
43
44
45
46 615 McClymont EL, Mauquoy D, Yeloff D, Broekens P, Van Geel B, Charman DJ., *et al.* 2008.
47
48 616 The disappearance of *Sphagnum imbricatum* from Butterburn Flow, UK. *Holocene* **18**: 991-
49
50 617 1002.
51
52
53
54
55
56
57
58
59
60

- 618 Meyers PA. 2003. Applications of organic geochemistry to paleolimnological
619 reconstructions: A summary of examples from the Laurentian Great Lakes. *Organic*
620 *Geochemistry* **34**: 261-289.
- 621 Moore TR, Bubier JL, Bledzki L. 2007. Litter decomposition in temperate peatland
622 ecosystems: The effect of substrate and site. *Ecosystems*, **10**: 949-963.
- 623 Nott CJ, Xie S, Avsejs LA, Maddy D, Chambers FM, Evershed RP. 2000. *n*-Alkane
624 distributions in ombrotrophic mires as indicators of vegetation change related to climatic
625 variation. *Organic Geochemistry* **31**: 231-235.
- 626 Oksanen PO, Kuhry P, Alekseeva RN. 2001. Holocene development of the Rogovaya River
627 peat plateau, European Russian Arctic. *Holocene* **11**: 25-40.
- 628 Ortiz JE, Díaz-Bautista A, Aldasoro JJ, Torres T, Gallego JLR, Moreno L, *et al.* 2011. *n*-
629 Alkan-2-ones in peat-forming plants from the Roñanzas ombrotrophic bog (Asturias,
630 northern Spain). *Organic Geochemistry* **42**: 586-592.
- 631 Ortiz JE, Gallego JLR, Torres T, Díaz-Bautista A, Sierra C. 2010. Palaeoenvironmental
632 reconstruction of Northern Spain during the last 8000 cal yr BP based on the biomarker
633 content of the Roñanzas peat bog (Asturias). *Organic Geochemistry* **41**: 454-466.
- 634 Pancost RD, Baas M, Van Geel B, Sinninghe Damsté JS. 2002. Biomarkers as proxies for
635 plant inputs to peats: An example from a sub-boreal ombrotrophic bog. *Organic*
636 *Geochemistry* **33**: 675-690
- 637 R Development Core Team (2012). R: A language and environment for statistical computing.
638 R Foundation for Statistical Computing, Vienna, Austria. <http://www.R-project.org/>.

1
2
3 639 Reimer PJ, Bard E, Bayliss A, Beck JW, Blackwell PG, Bronk Ramsey C, Buck CE, Cheng
4
5 640 H, Edwards RL, Friedrich M, Grootes PM, *et al.* 2013. IntCal13 and MARINE13 radiocarbon
6
7 641 age calibration curves 0-50000 years calBP. *Radiocarbon* **55**:1869-1887.
8
9
10
11 642 Repo ME, Susiluoto S, Lind SE, Jokinen S, Elsakov V, Biasi C, Virtanen T, Martikainen PJ.
12
13 643 2009. Large N₂O emissions from cryoturbated peat soil in tundra. *Nature Geoscience* **2**: 189-
14
15 644 192.
16
17
18
19 645 Ronkainen T, McClymont EL, Välranta M, Tuittila E-S. 2013. The *n*-alkane and sterol
20
21 646 composition of living fen plants as a potential tool for palaeoecological studies. *Organic*
22
23 647 *Geochemistry* **59**: 1-9.
24
25
26
27 648 Ronkainen T, McClymont EL, Tuittila E-S, Välranta M. 2014. Plant macrofossil and
28
29 649 biomarker evidence of fen–bog transition and associated changes in vegetation in two Finnish
30
31 650 peatlands. *Holocene in press* **24**: 828-841.
32
33
34
35 651 Routh J, Hugelius G, Kuhry P, Filley T, Kaislahti-Tillman P, Becher M, Crill P. 2014. Multi-
36
37 652 proxy study of soil organic matter dynamics in permafrost peat deposits reveal vulnerability
38
39 653 to climate change in the European Russian Arctic. *Chemical Geology* **368**: 104-117, ISSN
40
41 654 0009-2541, <http://dx.doi.org/10.1016/j.chemgeo.2013.12.022>.
42
43
44
45 655 Rydin H, Jeglum JK. 2006. *The Biology of Peatlands*. Oxford: Oxford University Press.
46
47
48 656 Sachse D, Radke J, Gleixner G. 2006. dD values of individual n-alkanes from terrestrial
49
50 657 plants along a climatic gradient - Implications for the sedimentary biomarker record. *Organic*
51
52 658 *Geochemistry* **37**: 469-483.
53
54
55
56 659 Salasoo I. 1987. Epicuticular wax alkanes of some heath plants in central Alaska.
57
58 660 *Biochemical Systematics and Ecology* **15**: 105–107
59
60

- 661 Seppälä M. 2003. Surface abrasion of palsas by wind action in Finnish Lapland.
662 *Geomorphology* **52**:141–148.
- 663 Speranza A, Van Der Plicht J, Van Geel B. 2000. Improving the time control of the
664 Subboreal/Subatlantic transition in a Czech peat sequence by ¹⁴C wiggle-matching.
665 *Quaternary Science Reviews* **19**: 1589-1604.
- 666 Strakova P, Niemi RM, Freeman C, Peltoniemi K, Toberman H, Heiskanen I, Laiho R. 2011.
667 Litter type affects the activity of aerobic decomposers in a boreal peatland more than site
668 nutrient and water table regimes. *Biogeosciences* **8**: 2741-2755.
- 669 Stuiver M, Reimer PJ. 1993. Extended ¹⁴C Data Base and Revised Calib 3.0 ¹⁴C Age
670 Calibration Program. *Radiocarbon* **35**:215-230.
- 671 Szumigalski AR, Bayley SE. 1996. Decomposition along a bog to rich fen gradient in central
672 alberta, canada. *Canadian Journal of Botany* **74**: 573-581.
- 673 Tarasov PE, Müller S, Zech M, Andreeva D, Diekmann B, Leipe C. 2013. Last glacial
674 vegetation reconstructions in the extreme-continental eastern Asia: Potentials of pollen and n-
675 alkane biomarker analyses. *Quaternary International* **290-291**: 253-263.
- 676 Tarnocai C, Canadell JG, Schuur EAG, Kuhry P, Mazhitova G, Zimov S. 2009. Soil organic
677 carbon pools in the northern circumpolar permafrost region. *Global Biogeochemical Cycles*
678 **23**: 11.
- 679 Tuittila E-S, Välijärvi M, Laine A, Korhola A. 2007. Controls of mire vegetation succession
680 in a southern boreal bog. *Journal of Vegetation Science* **18**: 891-902.

1
2
3
4
5
6
7
8
9
10
11
12
13
14
15
16
17
18
19
20
21
22
23
24
25
26
27
28
29
30
31
32
33
34
35
36
37
38
39
40
41
42
43
44
45
46
47
48
49
50
51
52
53
54
55
56
57
58
59
60

681 ter Braak CJFP, Šmilauer P. 2002. CANOCO reference manual and CanoDraw for Windows
682 user's guide: Software for canonical community ordination (version 4.5). NY, Ithaca:
683 Microcomputer Power.

684 Virtanen T, Ek M. 2013. The fragmented nature of tundra landscape. *International Journal of*
685 *Applied Earth Observation and Geoinformation* **27**: 4-12.

686 Väiliranta M, Kaakinen A, Kuhry P. 2003. Holocene climate and landscape evolution east of
687 the Pechora Delta, East-European Russian Arctic. *Quaternary Research* **59**: 335-344.

688 Väiliranta M, Korhola A, Seppä H, Tuittila E-S, Sarmaja-Korjonen K, Laine J, *et al.* 2007.
689 High-resolution reconstruction of wetness dynamics in a southern boreal raised bog, Finland,
690 during the late Holocene: A quantitative approach. *Holocene* **17**: 1093-1107.

691 Wheeler BD, Proctor MCF. 2000. Ecological gradients, subdivisions and terminology of
692 north-west European mires. *Journal of Ecology* **88**: 187-203.

693 Yu Z, Loisel J, Brosseau DP, Beilman DW Hunt SJ. 2010. Global peatland dynamics since
694 the last glacial maximum. *Geophysical Research Letters* **37**(13).

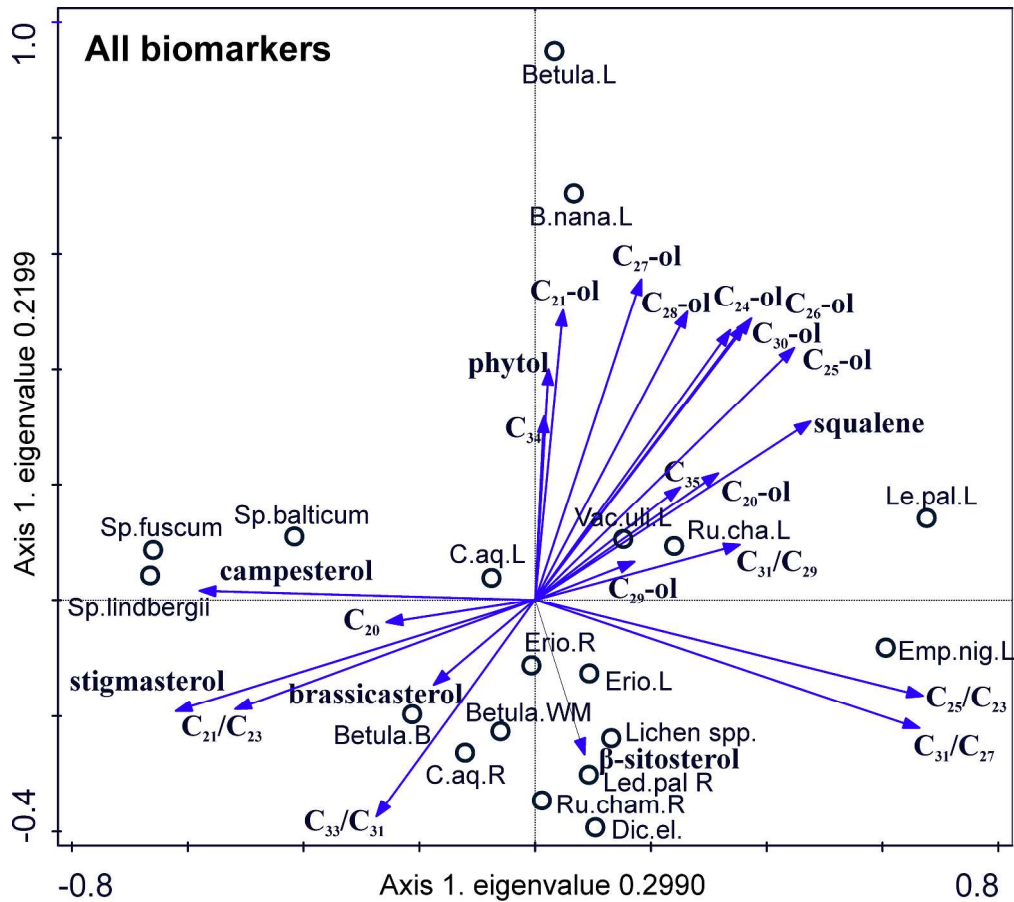
695 Yu Z, Loisel J, Turetsky MR, Cai S, Zhao Y, Froking S, *et al.* 2013. Evidence for elevated
696 emissions from high-latitude wetlands contributing to high atmospheric CH₄ concentration in
697 the early Holocene. *Global Biogeochem Cycles* **27**:131-40.

698 Xie S, Nott CJ, Avsejs LA, Volders F, Maddy D, Chambers FM, *et al.* 2000. Palaeoclimate
699 records in compound-specific δD values of a lipid biomarker in ombrotrophic peat. *Organic*
700 *Geochemistry* **31**: 1053-1057.

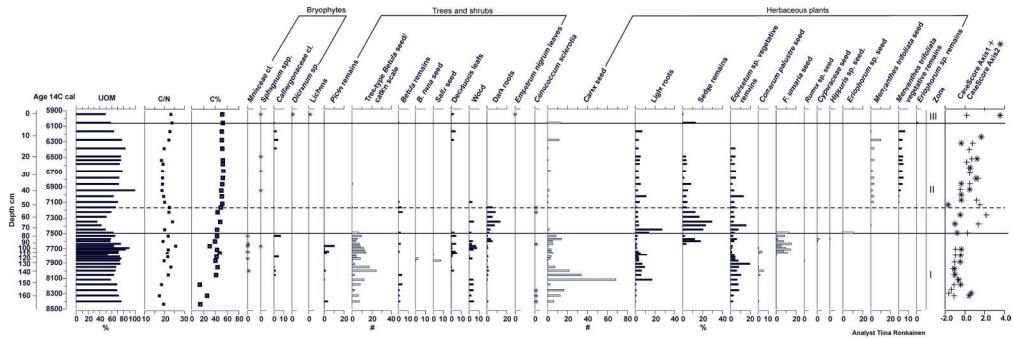
- 1
2
3 701 Zheng Y, Zhou W, Meyers PA, Xie S. 2007. Lipid biomarkers in the zongzi-hongyuan peat
4
5 702 deposit: Indicators of holocene climate changes in west china. *Organic Geochemistry* **38**:
6
7 703 1927-1940.
8
9
10
11 704 Økland RH, Okland T, Rydgren K. 2001. A Scandinavian perspective on ecological gradients
12
13 705 in north-west European mires: Reply to Wheeler and Proctor. *Journal of Ecology* **89**: 481-
14
15 706 486.
16
17
18
19
20
21
22
23
24
25
26
27
28
29
30
31
32
33
34
35
36
37
38
39
40
41
42
43
44
45
46
47
48
49
50
51
52
53
54
55
56
57
58
59
60



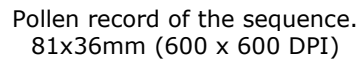
Map of the site and the bare peat circles. Maps produced by T. Virtanen; satellite image based on QuickBird
© DigitalGlobe; Distributed by Eurimage/Pöyry.
142x147mm (300 x 300 DPI)

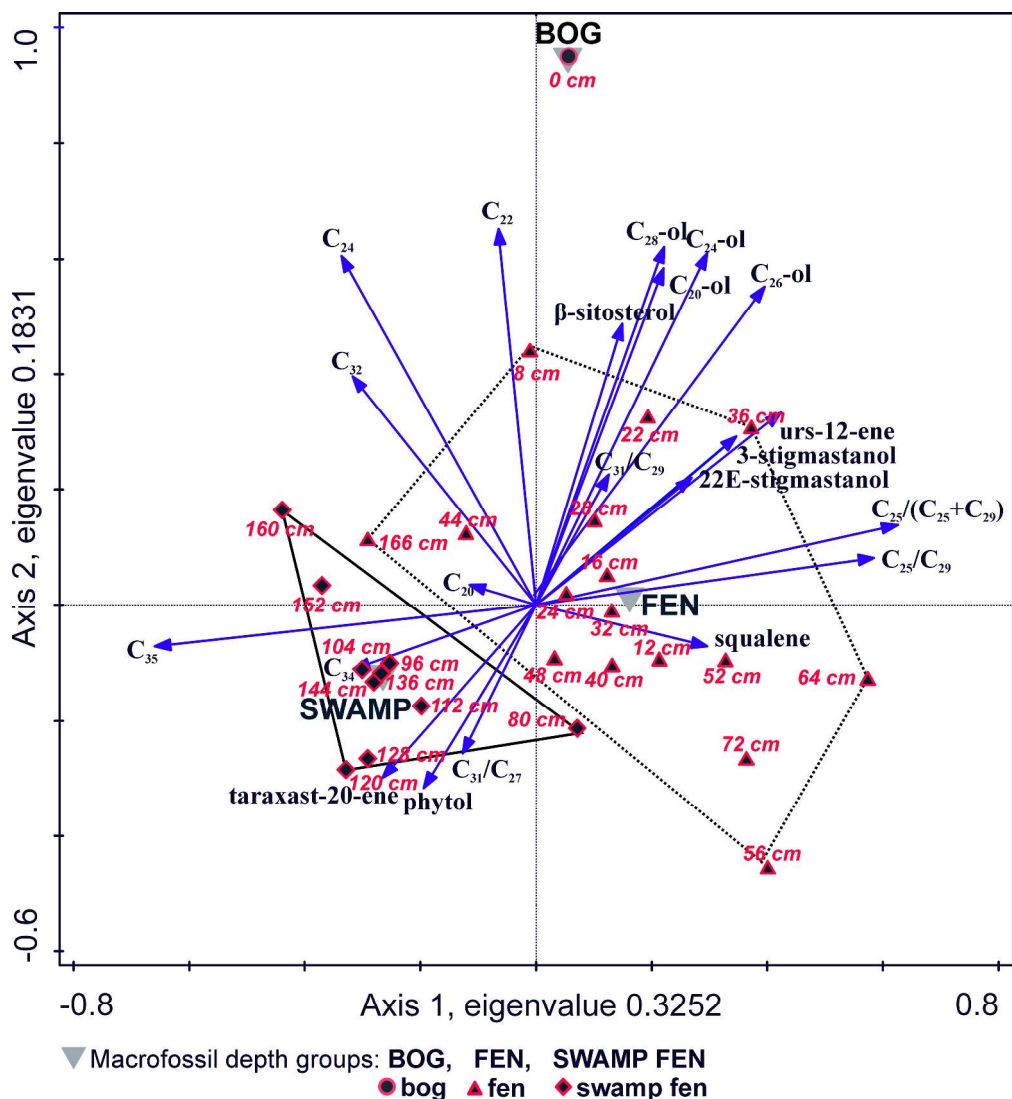


PCA of living plant biomarkers. All detected biomarkers combined first two axes explain 52% of the variation, in the figure 50% (n=23) best explaining biomarkers are shown.
165x147mm (600 x 600 DPI)



Plant macrofossils of the peat sequence. Black bars represent percentage coverages, grey bars represent counted values, macrofossils with star symbol the percentage coverage was 1 % or less. Ages are calibrated BP years. Marked zones I: swamp fen, II: fen, III: bog. Case score Axis 1 and 2 are case scores of axis 1 and 2 from peat biomarker PCA (Fig 5). Dashed line marks zone within fen zone where UOM is low and amount of sedges is high.
95x31mm (600 x 600 DPI)





PCA ordination of the biomarkers in the peat sequence. First two axes explain 51% of the variation. Biomarkers explaining 50% (n=23) of the variation are shown. Depth groups (swamp, fen, bog) derived from macrofossil TWINSPAN analyses are used as supplementary environmental variables.

Radiocarbon results and corresponding ages. Dated material is from bulk peat sample.

Lab code	Depth (cm)	14C age (14C yr BP \pm)	Calibrated age (cal yr BP, 95% probability)
Poz-53596	0	5220 \pm 1 σ 35	5930 - 5992
Poz-53598	26	5840 \pm 1 σ 40	6570 - 6727
Poz-53599	54	6300 \pm 1 σ 40	7176 - 7264
Poz-53600	82	6690 \pm 1 σ 40	7511 - 7592
Poz-54230	110	6960 \pm 1 σ 50	7719 - 7844
Poz-54231	138	7140 \pm 1 σ 40	7940 - 7997
Poz-54232	166	7670 \pm 1 σ 50	8410 - 8517

1
2
3
4
5
6
7
8
9
10
11
12
13
14
15
16
17
18
19
20
21
22
23
24
25
26
27
28
29
30
31
32
33
34
35
36
37
38
39
40
41
42
43
44
45
46
47
48
49
50
51
52
53
54
55
56
57
58
59
60

LEVEL 1	LEVEL 2
	n=11 Group 00
	Sample depth cm: 80, 88, 96, 104, 112, 120, 128, 136, 144, 152, 160
n=28	dark root, deciduous leaves, wood, <i>Picea</i> remains, <i>C. palustre</i> seeds, <i>Betula</i> seeds, <i>F. ulmaria</i> seeds
Sample depth cm: 4, 8, 12, 16, 22, 24, 28, 32, 36, 40, 44, 48, 52, 56, 64, 72, 80, 88, 96, 104, 112, 120, 128, 136, 144, 152, 160, 166	
<i>Calliergonaceae</i> , shrub root, light root, <i>Betula</i> remains, <i>Equisetum</i> veg. remains, <i>M. trifoliata</i> veg. remains, <i>Carex</i> seeds, <i>M. trifoliata</i> seeds, <i>Betula</i> seeds	n=17 Group 01
	Sample depth cm: 4, 8, 12, 16, 22, 24, 28, 32, 36, 40, 44, 48, 52, 56, 64, 72, 166
	sedge remains, <i>M. trifoliata</i> veg. remains, <i>M. trifoliata</i> seeds
n=1 Group 0	
Sample depth cm: 0	
<i>Sphagnum</i> spp., <i>Dicranum</i> spp., Lichen spp., <i>E. nigrum</i> , deciduous leaves, wood	
Division 1: n=29, eigenvalue 0.300	Division 2 (groups 00 and 01): n=28, eigenvalue 0.243

Plant samples		n- alkanes			
Sample	Habitat	C18	C19	C20	C21
<i>Betula</i> tree L	mineral soil	nd	nd	0.5	17.9
<i>B.nana</i> L	peat plateau hummock	nd	nd	0.2	6.3
<i>Rubus chameamorus</i> L	peat plateau hummock	nd	nd	0.7	1.5
<i>Carex aquatilis</i> L	fen	nd	0.8	0.6	3.8
<i>Eriophorum</i> sp. L	fen	nd	nd	0.4	4.8
<i>Vaccinium uliginosum</i> L	peat plateau hummock	nd	nd	nd	0.4
<i>Ledum palustre</i> L	peat plateau hummock	nd	nd	nd	0.9
<i>Empetrum nigrum</i> L	peat plateau hummock	nd	nd	nd	0.5
<i>B.nana</i> R	peat plateau hummock	nd	nd	0.2	0.3
<i>R. chameamorus</i> R	peat plateau hummock	nd	nd	0.1	0.3
<i>C.aquatilis</i> R	fen	nd	nd	0.2	0.9
<i>Eriophorum</i> s p. R	fen	nd	nd	0.3	2.6
<i>V. uliginosum</i> R	peat plateau hummock	nd	nd	nd	nd
<i>L. palustre</i> R	peat plateau hummock	nd	nd	0.3	0.9
<i>E. nigrum</i> R	peat plateau hummock	nd	nd	0.2	0.3
<i>Betula</i> tree WM	mineral soil	nd	0.1	0.2	0.6
<i>Betule</i> tree B	mineral soil	1.9	4.1	6.0	8.2
<i>Lichen</i> spp.	peat plateau hummock	nd	0.2	0.2	0.5
<i>Dicranum elongatum</i>	peat plateau hummock	nd	0.3	0.2	0.8
<i>Sphagnum fuscum</i>	peat plateau hummock	nd	0.3	0.2	86.9
<i>Sp.balticum</i>	fen	nd	2.1	0.6	38.7
<i>Sp.lindbergii</i>	fen	nd	0.7	0.2	20.2

Tree *Betula* = *Betula pubescens* ssp. *Czerepanovii*, syn. *Tortuosa*
not detected = nd
sample omitted = -
L = leaves
R = roots
WM = wood matter
B = bark

Supplementary information 1.
Plant biomarker data.

C22	C23	C24	C25	C26	C27	C28	C29	C30	C31	C32
21.0	1141.6	88.5	1510.2	96.6	2565.1	34.4	319.7	24.3	248.0	11.0
7.4	489.8	33.6	550.3	29.9	844.7	20.0	171.9	13.5	306.6	9.0
11.4	2.3	14.0	24.7	11.9	43.7	11.9	21.9	4.4	9.6	4.4
2.8	18.4	14.9	17.5	13.2	58.2	13.3	27.1	7.2	8.8	4.4
2.0	12.5	11.3	31.8	11.1	66.5	12.3	101.4	8.1	40.6	4.4
1.2	9.2	15.8	42.9	11.4	127.0	11.9	15.7	6.5	7.3	3.1
0.9	11.8	8.1	40.9	12.1	102.3	34.5	1448.0	66.1	1623.1	47.4
0.7	7.2	6.1	24.3	6.5	156.4	20.0	852.8	47.3	1552.3	40.5
0.7	2.9	4.7	5.2	4.2	6.9	6.3	7.2	4.9	5.9	2.9
1.2	4.3	8.0	8.5	7.7	10.9	7.6	10.7	6.1	8.1	2.7
1.5	6.6	10.8	11.5	11.0	13.9	9.6	10.4	6.2	5.8	3.5
2.5	14.1	14.0	24.9	16.7	45.6	18.9	40.1	13.4	20.0	9.6
1.3	4.4	8.4	8.4	8.6	10.0	11.3	10.0	7.8	8.1	4.2
1.0	4.6	7.7	10.1	10.6	12.0	10.0	17.2	6.9	15.1	4.1
0.8	2.5	5.3	5.5	5.3	8.2	7.0	68.8	3.5	46.4	2.5
1.6	6.7	7.3	12.1	7.0	15.9	13.4	9.1	4.9	4.2	3.3
5.7	9.2	11.4	14.4	9.3	24.3	8.0	10.7	8.9	7.8	5.0
1.2	4.0	7.6	10.3	11.2	15.7	12.3	24.9	9.6	31.8	4.9
1.0	4.0	8.3	9.6	8.6	10.5	5.8	34.4	5.6	59.3	3.2
4.1	103.5	11.5	133.6	11.2	59.5	5.0	11.8	2.1	9.4	1.5
3.7	66.4	14.1	44.2	18.4	33.2	28.2	27.4	24.0	21.0	13.5
2.8	45.4	8.1	21.8	8.7	11.7	7.9	7.8	4.1	4.8	2.8

			<i>n</i> - alkane ratios				
C33	C34	C35	C23/C25	C23/C27	C23/C29	C23/C31	C25/C29
21.3	6.6	2.6	0.8	0.4	3.6	4.6	0.6
29.7	1.2	0.8	0.9	0.6	2.8	1.6	0.7
4.5	2.2	1.7	0.1	0.1	0.1	0.2	0.6
3.1	2.7	1.6	1.0	0.3	0.7	2.1	0.3
5.3	3.5	2.0	0.4	0.2	0.1	0.3	0.5
3.3	1.8	1.4	0.2	0.1	0.6	1.3	0.3
355.0	2.4	1.9	0.3	0.1	0.0	0.0	0.4
539.9	3.7	2.2	0.3	0.0	0.0	0.0	0.2
2.1	1.3	0.9	0.6	0.4	0.4	0.5	0.7
3.3	1.5	0.9	0.5	0.4	0.4	0.5	0.8
3.1	2.0	1.1	0.6	0.5	0.6	1.1	0.8
6.0	4.9	2.1	0.6	0.3	0.4	0.7	0.5
2.9	2.1	0.9	0.5	0.4	0.4	0.5	0.8
3.3	1.3	1.6	0.5	0.4	0.3	0.3	0.8
3.5	1.2	0.7	0.5	0.3	0.0	0.1	0.7
1.7	1.9	1.1	0.6	0.4	0.7	1.6	0.8
3.4	2.9	1.4	0.6	0.4	0.9	1.2	0.6
9.2	2.8	2.0	0.4	0.3	0.2	0.1	0.7
11.6	1.5	0.8	0.4	0.4	0.1	0.1	0.9
2.3	1.6	0.5	0.8	1.7	8.8	11.0	2.2
9.5	6.9	4.7	1.5	2.0	2.4	3.2	1.3
2.2	1.9	0.9	2.1	3.9	5.8	9.4	1.9

C31/C27	C31/C29	C33/C31	C23/(C23+C29)	C25/(C25+C29)	C23/(C27+C31)
0.1	0.8	0.1	0.8	0.8	0.4
0.4	1.8	0.1	0.7	0.8	0.4
0.2	0.4	0.5	0.1	0.5	0.0
0.2	0.3	0.4	0.4	0.4	0.3
0.6	0.4	0.1	0.1	0.2	0.1
0.1	0.5	0.5	0.4	0.7	0.1
15.9	1.1	0.2	0.0	0.0	0.0
9.9	1.8	0.3	0.0	0.0	0.0
0.8	0.8	0.4	0.3	0.4	0.2
0.7	0.8	0.4	0.3	0.4	0.2
0.4	0.6	0.5	0.4	0.5	0.3
0.4	0.5	0.3	0.3	0.4	0.2
0.8	0.8	0.4	0.3	0.5	0.2
1.3	0.9	0.2	0.2	0.4	0.2
5.6	0.7	0.1	0.0	0.1	0.0
0.3	0.5	0.4	0.4	0.6	0.3
0.3	0.7	0.4	0.5	0.6	0.3
2.0	1.3	0.3	0.1	0.3	0.1
5.6	1.7	0.2	0.1	0.2	0.1
0.2	0.8	0.2	0.9	0.9	1.5
0.6	0.8	0.5	0.7	0.6	1.2
0.4	0.6	0.5	0.9	0.7	2.8

Paq	ACL C19-C35	Pwax	C23/C21	C21/C23	C25/C21	C25/C23
0.8	26.0	0.5	63.9	0.0	84.5	1.3
0.7	26.4	0.6	77.5	0.0	87.1	1.1
0.5	27.5	0.7	1.5	0.7	16.0	10.6
0.5	26.9	0.7	4.9	0.2	4.7	1.0
0.2	28.0	0.8	2.6	0.4	6.6	2.5
0.7	26.8	0.7	23.1	0.0	107.9	4.7
0.0	30.2	1.0	13.2	0.1	45.6	3.5
0.0	30.5	1.0	15.7	0.1	52.9	3.4
0.4	28.1	0.7	9.3	0.1	16.4	1.8
0.4	28.0	0.7	16.1	0.1	32.2	2.0
0.5	27.3	0.6	7.7	0.1	13.3	1.7
0.4	27.6	0.7	5.5	0.2	9.7	1.8
0.4	27.9	0.7		0.0		1.9
0.3	28.3	0.8	5.1	0.2	11.3	2.2
0.1	29.4	0.9	9.9	0.1	21.7	2.2
0.6	27.0	0.6	10.7	0.1	19.3	1.8
0.6	26.2	0.6	1.1	0.9	1.8	1.6
0.2	29.1	0.8	7.7	0.1	20.0	2.6
0.1	29.6	0.9	5.0	0.2	12.1	2.4
0.9	24.2	0.3	1.2	0.8	1.5	1.3
0.7	25.5	0.4	1.7	0.6	1.1	0.7
0.8	24.4	0.3	2.2	0.4	1.1	0.5

Sterol/triterpenoid						
squalene	taraxer-14-ene	phytol	brassicasterol	campesterol	stigmasterol	β -sitosterol
160.0	nd	nd	nd	nd	nd	70343.8
31.3	nd	nd	nd	nd	nd	6609.5
449.7	nd	nd	nd	nd	nd	2600.4
21.0	nd	nd	nd	212.7	nd	7707.1
16.3	nd	5209.0	nd	55.7	nd	nd
190.7	nd	7309.5	nd	827.5	246.2	17494.8
73.1	nd	4835.7	nd	704.8	214.6	6192.5
13.5	nd	284190.2	nd	nd	nd	139915.0
92.7	nd	nd	-	-	-	-
1.1	nd	1647.4	nd	28.0	nd	2989.5
9.1	nd	10575.3	nd	nd	nd	5210.3
18.0	nd	1460.4	68.1	nd	nd	3307.8
210.5	nd	-	-	-	-	-
211.1	nd	1215.3	68.6	3172.6	2791.0	3994.3
414.4	nd	-	-	-	-	-
327.2	nd	nd	nd	257.8	24.9	4814.4
13.9	nd	nd	nd	nd	nd	26757.1
nd	nd	828.1	2994.7	3831.5	10807.4	1546.6
nd	12.5	122409.4	nd	87996.1	70963.1	50805.9
nd	2.2	893.2	nd	nd	nd	288448.1
nd	nd	646.6	nd	nd	nd	54058.6
nd	nd	nd	nd	126.7	66.2	4348.4

	<i>n</i> - alcohols						
3-stigmastanol	C20-ol	C21-ol	C22-ol	C23-ol	C24-ol	C25-ol	C26-ol
1465.1	124.5	nd	nd	nd	79.9	nd	nd
290.4	nd	nd	nd	nd	nd	nd	nd
277.9	nd	nd	nd	nd	nd	nd	nd
673.1	nd	nd	nd	nd	213.6	nd	420.0
nd	242.6	18.5	1177.4	97.5	1153.0	nd	491.6
326.9	nd	nd	nd	nd	60.7	nd	108.9
131.9	nd	nd	nd	nd	86.7	nd	346.8
nd	1134.0	nd	2589.1	nd	11608.9	778.1	82238.3
-	-	-	-	-	-	-	-
80.0	26.5	nd	1792.0	73.1	768.3	61.5	346.3
nd	221.4	nd	135.8	11.9	864.1	33.6	619.2
nd	35.3	nd	101.6	nd	513.8	nd	386.8
-	-	-	-	-	-	-	-
nd	nd	nd	nd	nd	31.2	nd	nd
-	-	-	-	-	-	-	-
90.6	nd	nd	nd	nd	nd	nd	nd
nd	39.2	nd	nd	nd	nd	nd	nd
nd	nd	nd	nd	nd	nd	nd	nd
nd	nd	nd	nd	nd	3768.4	nd	4604.0
58609.5	1082.6	nd	nd	nd	nd	nd	nd
nd	nd	nd	nd	nd	nd	nd	nd
136.9	nd	nd	nd	nd	nd	nd	nd

C27-ol	C28-ol	C29-ol	C30-ol
nd	nd	nd	nd
nd	nd	nd	nd
nd	nd	nd	nd
nd	983.0	nd	1517.4
44.8	541.4	nd	66.3
nd	122.6	nd	nd
72.4	7457.9	nd	220.9
1981.1	52463.2	832.6	5781.2
-	-	-	-
56.8	326.0	nd	19.3
106.5	652.1	nd	nd
nd	191.9	nd	nd
-	-	-	-
nd	nd	nd	nd
-	-	-	-
nd	nd	nd	nd
nd	nd	nd	nd
nd	nd	nd	nd
nd	1467.6	nd	nd
nd	nd	nd	nd
nd	nd	nd	nd
nd	nd	nd	nd

Peat samples					Sterol/triterpenoid			
Depth	C%	C/N	Bulk density	CPI	squalene	taraxer-14-ene	urs-12-ene	taraxast-20-ene
0 cm	52.6	23.4	0.16	7.5	0.9	15.5	2.9	3.8
4 cm	53.0	24.0	0.15	7.1	0.3	7.9	2.8	4.0
8 cm	51.5	22.8	0.10	6.7	1.1	4.7	2.0	2.0
12 cm	51.1	22.3	0.09	5.3	2.2	nd	nd	1.6
16 cm	52.4	19.8	0.07	3.6	69.6	nd	5.4	2.0
22 cm	52.9	18.5	0.08	5.0	0.9	nd	2.2	3.3
24 cm	53.2	19.4	0.07	5.0	nd	nd	1.6	3.4
28 cm	54.0	19.0	0.10	4.9	1.1	nd	5.3	4.7
32 cm	53.0	19.2	0.09	4.6	0.5	nd	5.0	5.4
36 cm	52.2	19.0	0.12	3.3	0.6	nd	2.7	7.0
40 cm	50.6	18.9	0.09	4.8	0.3	nd	1.9	9.2
44 cm	51.6	19.7	0.14	2.2	1.0	nd	2.0	10.0
48 cm	52.3	20.1	0.07	4.4	0.5	nd	2.5	7.7
52 cm	49.7	22.5	0.00	3.8	2.1	nd	1.6	4.3
56 cm	44.1	22.2	0.08	2.4	1.9	nd	1.5	4.4
64 cm	48.5	24.1	0.07	2.3	2.3	nd	nd	6.5
72 cm	43.4	20.2	0.06	3.2	0.9	nd	0.9	5.3
80 cm	43.4	21.9	0.08	10.9	1.2	nd	2.7	4.8
88 cm	39.6	19.4	0.06	3.2	0.7	nd	2.3	8.1
96 cm	31.0	25.7	0.16	6.1	0.7	nd	nd	7.7
104 cm	43.1	22.1	0.08	6.7	1.0	nd	4.2	10.8
112 cm	47.6	21.4	0.08	6.4	1.6	nd	nd	11.3
120 cm	42.7	21.9	0.08	5.3	0.8	nd	nd	8.1
128 cm	40.7	19.9	0.08	5.9	1.1	nd	nd	4.6
136 cm	44.1	23.5	0.10	6.6	1.1	nd	nd	5.4
144 cm	42.0	22.1	0.09	3.3	0.7	nd	nd	7.5
152 cm	14.3	18.5	0.25	3.2	nd	nd	nd	4.6
160 cm	26.7	17.6	0.18	3.2	nd	nd	nd	5.3
166 cm	14.9	19.5	0.00	4.7	nd	nd	nd	3.4

not detected = nd
sample omitted = -
C22-ol concentrations are omitted from the analysis due contamination of the detected peak in GC-MS

Supplementary information 2.
Peat biomarker data.

phytol	campestrol	campestanol	stigmasterol	22E-stigmasterol-22-en-3 β -ol	β -sitosterol	3-stigmastanol	3-stigmastanol/ β -sitosterol
nd	1388.7	nd	663.5	nd	10791.6	2107.7	0.2
-	-	-	-	-	-	-	
136.1	244.4	nd	71.9	nd	2735.2	699.4	0.2
34.8	106.1	56.4	nd	nd	686.4	272.1	0.3
178.9	136.1	87.5	nd	nd	808.6	522.5	0.4
915.6	301.9	229.2	nd	nd	3064.6	1481.2	0.3
156.4	113.5	99.2	nd	nd	769.5	485.9	0.4
296.1	175.2	131.6	nd	nd	1012.0	886.5	0.5
165.6	129.4	73.5	nd	nd	663.3	610.5	0.5
536.2	202.2	186.2	88.3	135.1	1187.6	986.6	0.5
140.2	85.7	59.5	nd	nd	659.4	671.6	0.5
150.9	101.7	nd	nd	nd	528.5	459.7	0.5
336.8	nd	nd	nd	nd	1043.1	911.0	0.5
159.2	434.1	nd	nd	nd	14020.1	2604.5	0.2
12.7	42.6	35.8	nd	nd	787.3	500.5	0.4
113.0	420.4	293.8	nd	nd	2782.2	2331.1	0.5
98.7	214.1	113.5	nd	nd	1006.3	1135.7	0.5
345.3	nd	nd	nd	nd	1540.7	891.9	0.4
-	-	-	-	-	-	-	
374.7	nd	nd	nd	nd	2483.6	2206.6	0.5
227.9	nd	nd	nd	nd	612.1	425.5	0.4
453.7	nd	nd	nd	nd	1202.9	952.6	0.4
169.4	nd	nd	nd	nd	521.1	393.3	0.4
148.4	135.8	nd	nd	nd	804.4	464.0	0.4
162.6	nd	nd	nd	nd	1478.6	630.3	0.3
148.7	nd	nd	nd	nd	1013.2	659.2	0.4
440.0	nd	nd	nd	nd	4281.2	961.5	0.2
142.5	nd	nd	nd	nd	1813.4	693.6	0.3
104.8	nd	nd	nd	nd	913.9	372.8	0.3

1
2
3
4
5
6
7
8
9
10
11
12
13
14
15
16
17
18
19
20
21
22
23
24
25
26
27
28
29
30
31
32
33
34
35
36
37
38
39
40
41
42
43
44
45
46
47
48
49
50
51
52
53
54
55
56
57
58
59
60

n- alcohols

C20-ol	C21-ol	C22-ol	C23-ol	C24-ol	C25-ol	C26-ol	C27-ol	C28-ol
1284.0	405.4	-	707.1	5392.6	313.1	3387.5	360.1	2884.8
-	-	-	-	-	-	-	-	-
344.3	80.9	-	106.3	1046.0	46.1	679.1	62.1	478.6
37.0	5.2	-	nd	63.1	nd	49.5	nd	58.6
48.0	14.6	-	14.7	110.6	nd	126.2	nd	124.8
300.6	69.2	-	nd	1671.3	88.9	1160.8	90.5	715.9
45.0	10.4	-	nd	90.2	nd	86.1	nd	72.8
79.4	11.9	-	15.4	222.0	nd	189.2	nd	140.2
29.6	7.9	-	nd	81.6	nd	89.8	nd	97.3
168.5	32.7	-	43.0	1511.3	51.3	1355.6	53.0	978.3
27.1	15.1	-	nd	80.9	nd	143.5	nd	127.5
24.0	20.0	-	nd	55.4	nd	81.1	nd	93.3
nd	nd	-	nd	165.6	nd	248.2	nd	193.7
144.5	nd	-	nd	397.6	nd	282.4	nd	467.5
8.9	nd	-	nd	nd	nd	nd	nd	nd
103.1	190.7	-	491.9	35.7	nd	233.8	190.7	181.5
105.8	15.3	-	14.1	144.7	nd	120.2	nd	227.8
28.2	nd	-	nd	74.4	nd	69.5	nd	86.7
-	-	-	-	-	-	-	-	-
50.6	nd	-	nd	97.5	nd	nd	nd	149.1
41.5	nd	-	nd	35.4	nd	37.9	nd	45.6
44.3	nd	-	nd	47.5	nd	54.3	nd	76.8
18.1	nd	-	nd	37.3	nd	30.4	nd	39.9
30.3	nd	-	nd	31.9	nd	44.1	nd	37.9
32.1	nd	-	nd	63.9	nd	76.7	nd	128.4
33.5	nd	-	nd	60.0	nd	84.3	nd	72.5
nd	nd	-	nd	nd	nd	nd	nd	nd
76.4	nd	-	nd	95.2	nd	71.8	nd	149.5
426.5	nd	-	nd	nd	nd	nd	nd	297.0

C30-ol

274.2

-

55.2

nd

nd

120.3

nd

74.1

23.6

167.9

nd

nd

nd

nd

nd

nd

41.3

nd

-

nd

nd

nd

nd

nd

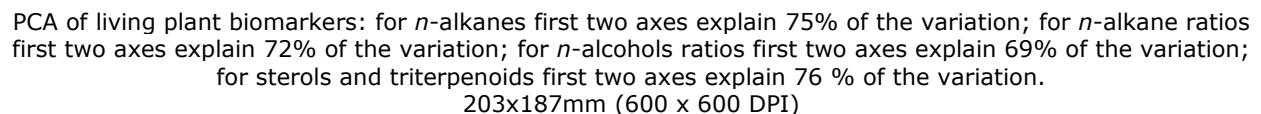
nd

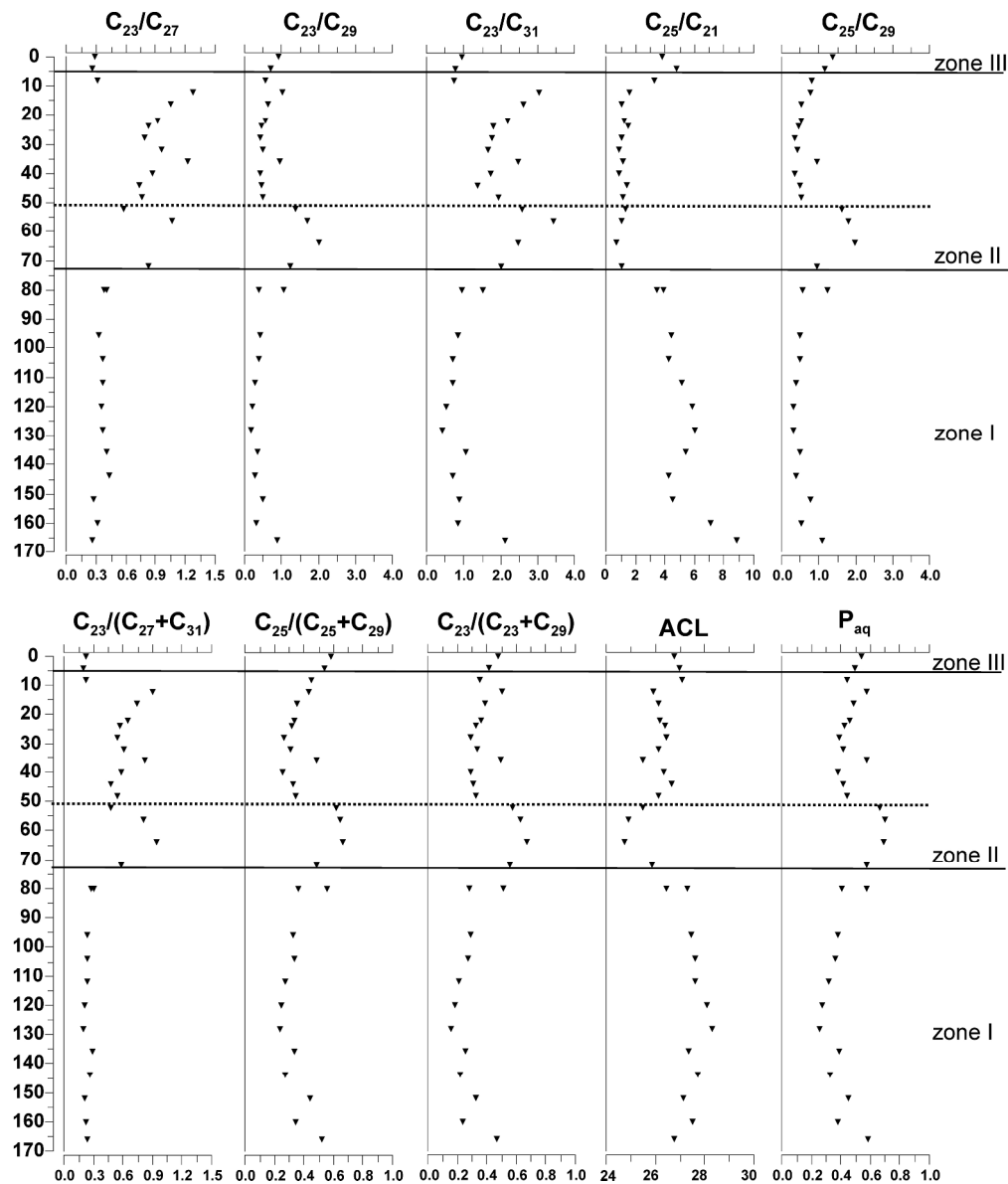
nd

nd

nd

nd





10 best fitted (PCA for peat ratios) *n*-alkane ratios of peat sequence. Marked zones according to the macrofossil data; I: swamp fen, II: fen, III: bog. Dashed line marks zone within fen zone where UOM is low and amount of sedges is high
182x214mm (600 x 600 DPI)